EUROPEAN ORGANIZATION FOR NUCLEAR RESEARCH
European Laboratory for Particle Physics

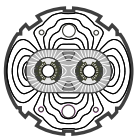

Large Hadron Collider Project **LHC Project Report 1012**

A semi-analytical method to generate an arbitrary 2D magnetic field and determine the associated current distribution

Stéphane Fartoukh

Abstract

This reports describes a novel method based on polynomial algebra techniques which aims to determine the transverse position of N current wires perpendicular to a plane in which the induced 2D magnetic field map shall exhibit a given multipole expansion at one or several specified locations. Rather than a case-by-case comparative study of the method with other existing ones, we will insist on the details of the method itself and then illustrate its potential to the design of many magnet classes, from very pure $2N$-pole magnets to more exotic components producing a magnetic field with more complex characteristics, such as FFAG magnets, mass-less septa or magnetic collimators.

Administrative Secretariat
LHC Division
CERN
CH-1211 Geneva 23
Switzerland

Geneva, September 2007

1 Introduction and initial motivation

In the context of the different possible scenarios for upgrading the LHC experimental insertions, flat beam optics options have been considered in order to enhance the machine luminosity. Assuming the beam to be flat in the horizontal plane at the interaction point (IP), $\beta_x^* \gg \beta_y^*$, it is well-known that low-β doublets with symmetric powering with respect to the IP are particularly well-suited to produce an arbitrarily small beam aspect ratio, $R_{\rm asp}^2 \equiv \beta_y^*/\beta_x^*$. This is indeed the case provided that, on both sides of the IP, the first and second quadrupoles of the doublet are focusing and defocusing, respectively, in the plane of smallest β^* in order to keep within reasonable bounds the peak β-function, $\beta_{\rm max}$, which is reached in the first quadrupole of the doublet. In the case of the LHC (proton-proton collision), and to pursue this option, it was then customarily agreed that the only possible way was to use two-in-one-aperture quadrupoles with **opposite gradients** in the two magnet bores, therefore requesting an early beam separation with the separation dipole D1 installed in between the doublet and the interaction point. Finally, with the significant increase of l^* needed to accommodate the D1, this so-called "dipole-first scenario" [1] was found to be less attractive in terms of $\beta_{\rm max}$ when comparing with other options using the present conceptual design of the LHC insertions with the low β-quadrupoles in front of the D1 (see e.g. [2] using the so-called "quadrupole-first" layout).

In view of these facts, we have then decided to try designing a new class of magnets, possessing a **single aperture** but generating, or approaching as close as possible, the left/right focusing/defocusing quadrupolar field that the twin quadrupole magnet described here-above would produce but, this time, in a "quadrupole-first scenario". As described in section 4.1, such a field can indeed be obtained, in several different manners and with a rather limited numbers of wires, for instance 2×10 wires if the multipole expansion of the produced magnetic field is requested to be purely quadrupolar up to $(a_{10},\, b_{10})$ around two specified horizontal positions $\pm x_0$ of the magnet aperture. In the usual complex notations, this can be expressed as:

$$\mathbf{B}(\pm x_0 \,+\, z) \equiv [B_y + i\, B_x]\,(\pm x_0 \,+\, x + i\, y) = \pm B_2\, z \,+\, \mathrm{O}(z^{11})\,, \tag{1}$$

that is a sort of combined dipole-sextupole magnet, with a vertical dipole field $B_1 \equiv -B_2 x_0$ at its center but for which the sextupolar component would exhibit straight and not parabolic asymptotic branches (i.e. $B_y(x) \,\propto\, |x|$ and not $B_y(x) \,\propto\, x^2$). The problem lies in the fact than when trying to push the gradient of this "sextupole-like quadrupole" to useful values for the LHC insertions, that is by stacking different layers of wires, each of them producing its own quadrupolar gradient $\pm B_2$ at the specified locations $\pm x_0$, the density of wires growths up very rapidly at certain accumulation points located in the magnet mid-plane. Then we converge slowly toward a two-in-one quadrupole design with a infinitely thin plate made of superconducting material separating the two magnet apertures and in which the density of current would become "infinite".

While we are now convinced that the aim initially pursued is not reachable, certainly not due to the method used, but rather due to some topological limitations linked to the harmonic properties of the magnetic field itself, we believe that it is nevertheless worth documenting our approach,

- which is new to our knowledge,
- and might have other applications to help in the design of more exotic magnets such as, for instance, FFAG magnets, mass-less septa and magnetic collimator, that is, in other words, single-bore magnets producing a magnetic field with a pre-defined multipole expansion at one or more than one transverse locations inside their aperture.

The method, based on polynomial algebra techniques will be fully described in Section 2. Already at this stage, the cases considered will be split into two distinct categories: the so-called

"unipolar-current magnets" in which the current is the same and has the same sign, say positive, in all the wires and the "bipolar-current magnets" for which the current is assumed to be negative for half of the wires.
In Section 3, the method will be applied for designing very pure $2N$-pole magnets (see section 3.1 and 3.2 for unipolar and bipolar-current magnets). The design of combined magnets (i.e. with more than one non-zero multipole components but still specified at one single transverse location inside the magnet aperture), will be illustrated in section 3.3 by dealing with the case of a combined dipole-quadrupole magnet. Unipolar and bipolar-current magnets will then be briefly compared in section 3.4. Finally, as mentioned above in the case of the "sextupole-like quadrupole", different wire stacking strategies needed to increase the magnitude of the induced magnetic field, will be discussed in detail in section 3.5 and illustrated only by a few examples in order to keep the length of the paper within reasonable bounds.
In Section 4, we will then address the more delicate problem of designing single-aperture magnets for which the constraints on the multipole expansion of the produced magnetic field are imposed at more than one location of the transverse plane. As possible examples, the "sextupole-like quadrupole" described above will be discussed in detail (see section 4.1). We will also present the cases of single aperture magnets where the multipole field expansion is vanishing (up to some order) at one location and can be approximated by a very pure dipole field at one or two other locations inside the magnet aperture (see section 4.2): that is no more no less than a mass-less septum or a two jaw magnetic collimator with relatively thin small transition between the zero-field and the dipole field regions.

2 Description of the method

2.1 Biot-Savart law for filamentary wires

We consider N wires of current I_n, parallel to each other and crossing the transverse plane $(x-y)$ at the positions $z_n \stackrel{\text{def}}{=} x_n + i\,y_n$. Using the Biot-Savart law, it is well-known that the produced magnetic field is purely two-dimensional. In complex notations it is given by

$$\mathbf{B}(z) \stackrel{\text{def}}{=} B_y(x+iy) + i\,B_x(x+iy) = \sum_{n=1}^{N} \frac{I_n}{z-z_n}\,, \tag{2}$$

considering $\mu_0 = 2\pi$ which will be assumed in all the rest of the paper except when numerical estimates will be needed.

2.2 Definition of the problem

Generally speaking, the problem is to determine the position of the N wires, that is finding the complex numbers $(z_n)_{1\le n\le N}$, such that the magnetic field they induced has a given multipole expansion at one or more than one specified locations, $(Z_p)_{1\le p\le P}$, of the transverse plane:

$$\mathbf{B}(z) \equiv \sum_{k=1}^{M_p} C_k^{(p)}\ (z-Z_p)^{k-1} + \mathbf{O}\left[(z-Z_p)^{M_p}\right]\ ,\ 1\le p\le P\,, \tag{3}$$

where the multipole expansion of the magnetic field at the position Z_p is specified up the order M_p and given by the complex harmonics $C_k^{(p)} \equiv B_k^{(p)} + iA_k^{(p)}$, $1\le k\le M_p$ (with $B_k^{(p)}$ and $A_k^{(p)}$ denoting the well-known normal and skew harmonics of order k at the transverse position $z=Z_p$). Strictly speaking, with our present and future conventions, $\mu_0 = 2\pi$ and the currents I_n which will be chosen equal to ± 1 (see sub-sections 2.3.1 and 2.3.2), the multipole components

$C_k^{(p)}$ will have to be specified in units of $\left[m^{-k}\right]$. In order to preserve the clarity of the text, this will however never be explicitly mentioned but will be kept in mind when numerical estimates will be needed.
This being said, noting that the complex harmonics $C_k^{(p)}$ are directly linked to the $k^{\rm th}$ derivatives of the magnetic field $\mathbf{B}(z)$ at the location $z = Z_p$, an approach would consist in writing the above conditions as follows:

$$C_k^{(p)} = \frac{1}{(k-1)!}\left(\frac{d^{k-1}\mathbf{B}}{dz^{k-1}}\right)(z=Z_p) \overset{\text{Eq. (2)}}{=} -\sum_{n=1}^{N}\frac{I_n}{(z_n-Z_p)^k}\,, 1\leq p\leq P,\, 1\leq k\leq M_p\,, \tag{4}$$

that is a set of $N' = \sum_{p=1}^{P} M_p$ highly non-linear equations to be solved in terms of the $2N$ variables of the problem, $(I_n, z_n)_{1\leq n\leq N}$ (being said that the matching between the number N' of constraints and the number of free variables will only be done at a later stage).

2.3 Generating Polynomials

This approach was typically that used in Ref. [3], being noted that a mixture of cartesian and cylindrical coordinates formalism was used in this article, rather than the complex formalism which has been used so far for reasons which will become obvious later on. Solving numerically the above set of Equations was indeed found efficient, for instance to exhibit the existence of so-called "unipolar-current magnets" for which all the currents I_n points in the same direction contrary to more conventional configurations where half of the wires has the other polarity. However, rather than passing directly to the numerical resolution, we will show that it is worth going a bit deeper into the formalism in order to set up a much faster and more constructive method to solve our problem.
The next step is indeed to introduce the following generating function:

$$\mathcal{G}(z) \overset{\text{def}}{=} \prod_{n=1}^{N}(1-z/z_n)^{I_n}\,. \tag{5}$$

In particular, we have

$$\mathcal{G}(0) = 1 \text{ and } \mathcal{G}(z_n) = 0\,,\ 1\leq n\leq N. \tag{6}$$

In the case where all the currents I_n are positive integers (unipolar-current magnets), the generating function $\mathcal{G}(z)$ has to be interpreted as a polynomial in the z-variable possessing N roots $z_1,\,\ldots,\,z_n$ of multiplicity $I_1,\,\ldots,\,I_n$, that is the N currents and wire positions to be determined. On the other hand, in the case where some of the current are negative integers, we will then have to deal with polynomial fractions rather than with simple polynomials.
This being said, the idea is to find certain functional relations fulfilled by the generating function $\mathcal{G}(z)$, rather than using directly a numerical method to solve the non-linear equations (4). For this purpose, it is worth noting that the magnetic field $\mathbf{B}(z)$ defined in Eq. (2) is simply given by the logarithmic derivative of the function $\mathcal{G}$:

$$\frac{\mathcal{G}'(z)}{\mathcal{G}(z)} = \frac{-1}{\prod_{k=1}^{N}(1-z/z_k)^{I_k}}\sum_{n=1}^{N}\left[\frac{I_n}{z_n}(1-z/z_n)^{I_n-1}\prod_{k\neq n}(1-z/z_k)^{I_k}\right] = \sum_{n=1}^{N}\frac{I_n}{z-z_n} \overset{\text{Eq. (2)}}{=} \mathbf{B}(z)\,. \tag{7}$$

Thanks to this observation, we can reformulate the condition (3) as follows:

$$\mathbf{B}(z) = \frac{\mathcal{G}'(z)}{\mathcal{G}(z)} \equiv \sum_{k=1}^{M_p} C_k^{(p)} \ (z - Z_p)^{k-1} + \mathrm{O}\left[(z - Z_p)^{M_p}\right]$$

$$\Longrightarrow \quad \frac{\mathcal{G}(Z_p + z)}{\mathcal{G}(Z_p)} = \exp\left[\sum_{k=1}^{M_p} \frac{C_k^{(p)}}{k} z^k\right] + \mathrm{O}\left(z^{M_p+1}\right) \stackrel{\text{def}}{=} R_p(z) + \mathrm{O}\left(z^{M_p+1}\right) \ , \ 1 \leq p \leq P \,, \tag{8}$$

where the generating function $\mathcal{G}(z)$ is the unknown and the functions $R_p(z)$ are polynomials of degree M_p given by the development in series of the exponential term up the order M_p:

$$R_p(z) \stackrel{\text{def}}{=} \exp\left[\sum_{k=1}^{M_p} \frac{C_k^{(p)}}{k} z^k\right] + \mathrm{O}\left(z^{M_p+1}\right) = \sum_{n=0}^{M_p} \left[\sum_{\substack{i_1 \ \ldots \ , i_{M_p} \\ \sum_{m=1}^{M_p} m\, i_m \equiv n}} \prod_{k=1}^{M_p} \frac{\left(C_k^{(p)}\right)^{i_k}}{k^{i_k}\, i_k!} \right] z^n \,. \tag{9}$$

In particular we have

$$R_p(0) = 1 \,. \tag{10}$$

For the sake of simplicity, but without losing any generality, we will assume that the multipole expansion of the magnetic field is specified up to the same order M for all the positions Z_p:

$$M_p \equiv M \ \ \Rightarrow \ \ \deg\left(R_p\right) = M \,, \ 1 \leq p \leq P \,. \tag{11}$$

Then, we will restrict ourselves to the following two specific cases.

2.3.1 Unipolar-current magnets

The magnets for which all the current I_n are positive and equal to unity will be referred as unipolar-current magnets. In this case, with a multipole field expansion specified up to the order M at each of the P distinct positions $(Z_p)_{1 \leq p \leq P}$ of the magnet aperture, the minimum number of wires needed is equal to $N \equiv M \times P$. In the case of unipolar magnets, as already mentioned, the generating function $\mathcal{G}(z)$ is a simple polynomial of degree N. Then, using the above formalism, the method is the following:

– **Step 1** first determine the polynomial

$$\mathcal{G}(z) \equiv Q_+(z) \stackrel{\text{def}}{=} \prod_{n=1}^{N} (1 - z/z_n^+) \stackrel{\text{def}}{=} 1 + \sum_{k=1}^{N} q_k^+ \, z^k \tag{12}$$

of degree $N \equiv M \times P$ which fulfills the P functional relations

$$Q_+(Z_p + z) \equiv Q_+(Z_p) \times R_p(z) \ + \ \mathrm{O}\left(z^{M+1}\right) \ , \ 1 \leq p \leq P \,, \tag{13}$$

where the polynomials R_p of degree M are given and depend on the P locations Z_p where the first M harmonics of the field are specified (see Eq. (9)). The above equation is clearly linear in the unknown Q_+. Said differently, by projecting the above condition onto the monomial basis $(1, z, \ldots, z^M)$ at each of the P specified locations Z_p, Eq. (13) can be expressed as a linear system of $P \times (M+1)$ equations with $N+1 \equiv P \times M + 1$ unknowns which are the $N+1$ coefficients of the polynomial $Q_+(z)$. However, using $Q_+(0) = R_p(0) = 1$ for all p (see Eq.'s (10) and (12)), the relation (13) can be reduced to

a determined system of $N = P \times M$ independent linear equations in the N coefficients $(q_n^+)_{1\leq n\leq N}$:

$$\sum_{k=m}^{N} \frac{k!\, Z_p^{k-m}}{(k-m)!}\, q_k^+ \;-\; R_p^{(m)}(0) \sum_{k=1}^{N} Z_p^k\, q_k^+ \equiv R_p^{(m)}(0),\; 1 \leq m \leq M,\; 1 \leq p \leq P, \quad (14)$$

with $R_p^{(m)}(0)$ the m^{th} derivative of the polynomial R_p at $z = 0$.

– **Step 2** in a second time, the transverse location of the N wires will be simply obtained by determining the complex roots $(z_n^+)_{1\leq n\leq N}$ of the generating polynomial Q_+.

To summarise, in the case of unipolar-current magnets, the proposed formalism transforms the initial non-linear system of N equations (see the conditions (4)) into a linear system to determine the N coefficients of a polynomial $Q_+(z)$ of degree N (with $Q_+(0) = 1$), the roots of which are the solutions of the problem.

The most convincing example of the powerfulness of the method can be illustrated in the case where the multipole expansion of the field is specified at one single location of the transverse plane, for instance to be dipolar up to an order M , i.e. $P = 1$, $N = M$, $Z_1 \equiv 0$, $C_1^{(1)} \equiv 1$ and $C_k^{(1)} \equiv 0$, $2 \leq k \leq M$. In this case, Eq. (13) is a strict equality since the the polynomial R_1 and Q_+ have the same degree $N = M$ and step 1 is straightforward:

$$R_1(z) \overset{\text{Eq. (9)}}{=} \exp(z) + \mathbf{O}(z^{M+1}) \Rightarrow Q_+(z) \overset{\text{Eq. (13)}}{=} \underbrace{Q_+(0)}_{\equiv 1}\, R_1(z) \equiv \sum_{k=0}^{M} \frac{z^k}{k!}\,. \quad (15)$$

Finding the M roots of the above polynomial leads to the C-shape unipolar-current dipole which was obtained by a purely numerical method in Ref. [3] and is illustrated in Fig. 1(a). The case of an arbitrary $2p$-pole will then follow immediately by finding the roots of the truncated series of $\exp(z^p/p)$, rather than that of $\exp(z)$. These simple cases will form the subject of Section 3.1.

2.3.2 Bipolar-current magnets

The magnets for which the sum of the currents I_n is equal to zero will be referred as bipolar-current magnets. For the sake of simplicity, half of the currents will be assumed to be positive and equal to unity while the other half set to -1. In particular, with a multipole field expansion specified up to the order M at each of the P distinct positions $(Z_p)_{1\leq p\leq P}$ of the magnet aperture, the minimum number of wires needed will be assumed to be an even integer equal to $N = M \times P \equiv 2\,N'$.

In this second case, the generating function $\mathcal{G}$ introduced in Eq. (5) becomes a polynomial fraction and is expressed in the following way:

$$\mathcal{G}(z) \equiv \frac{Q_+(z)}{Q_-(z)} \text{ with } Q_\pm(z) \overset{\text{def}}{=} \prod_{n=1}^{N'} (1 - z/z_n^\pm) \overset{\text{def}}{=} 1 + \sum_{k=1}^{N'} q_k^\pm\, z^k\,, \quad (16)$$

with $(z_n^\pm)_{1\leq n\leq N'}$ being the N' transverse positions of the wires with positive and negative currents, respectively. In particular, noting that two wires with opposite currents cancel obviously each other if positioned at the same location, these two sets of roots can be assumed strictly distinct. In other words, this means that the polynomials Q_+ and Q_- are necessarily coprime:

$$Q_+ \wedge Q_- = 1\,. \quad (17)$$

This being said, in the bipolar-current configuration, the relation (8) reads

$$Q_+(z+Z_p) = \lambda_p\, R_p(z) \times Q_-(z+Z_p) + \mathrm{O}(z^{M+1}) \text{ with } \lambda_p \equiv \frac{Q_+(Z_p)}{Q_-(Z_p)},\ 1 \le p \le P\,. \quad (18)$$

As in the unipolar case, the polynomials R_p are given (see Eq. (9)) and the number of unknowns is equal to $N = P \times M \equiv 2\,N'$ which are the monomial coefficients $(q_n^{\pm})_{1\le n\le N'}$ of the polynomials $Q_\pm$ (reminding that, by construction, $q_0^{\pm} = Q_\pm(0) = 1$). The total number of constraints is also equal to N (more precisely, $P\times(M+1)$ constraints when projecting onto the monomial basis $(1,\,\ldots,\,z^M)$ at each of the P specified locations Z_p but noting that P constraints are automatically fulfilled via $R_p(0) = 1$ and the above definition for the quantities λ_p).
However, contrary to the unipolar case, this set of conditions is not linear in the polynomials $Q_\pm$. In the case of an arbitrary number P of specified locations Z_p and without assuming any specific symmetry in the multipole expansion of the field at those locations, no general algorithm (other than a direct numerical approach) has been found so far to solve the problem. Nevertheless, if we restrict ourself to the most interesting cases $P = 1$ and $P = 2$, we will show hereafter that the problem can still be solved using standard linear algebra techniques.

Case $P = 1$. In this paragraph, the multipole field expansion is specified up to the order M at one single location $Z_1 = 0$ of the transverse plane. $M \equiv 2\,m$ is assumed to be an even integer and the field harmonics specified at $z = 0$ are noted $(C_k)_{1\le k\le 2m}$. According to the relation (18), the problem is to find the two polynomials of degree $N' = M/2 = m$ which fulfill the following constraints:

$$Q_+(z) \equiv \underbrace{\frac{Q_+(0)}{Q_-(0)}}_{\equiv 1} \times Q_-(z)\, R(z) + \mathrm{O}(z^{2m+1}) = Q_-(z)\, R(z) + \mathrm{O}(z^{2m+1})\,, \quad (19)$$

with $R(z)$ the polynomial of degree $2m$ defined by

$$R(z) \stackrel{\text{def}}{=} \exp\left[\sum_{k=1}^{2m} \frac{C_k}{k}\, z^k\right] + \mathrm{O}(z^{2m+1}) = 1 + \sum_{k=1}^{2m} \frac{C_k}{k}\, z^k + \ldots \stackrel{\text{def}}{=} 1 + \sum_{n=1}^{2m} r_n\, z^n\,. \quad (20)$$

The condition (19) can then be solved in two steps.

- **Step 1-a** Reminding that the polynomial Q_+ is of degree m and using $Q_-(0) \equiv q_0^- = 1$, the projection of Eq. (19) onto the basis $(z^{m+1}\,,\ldots\,,z^{2m})$ gives

$$\sum_{k=0}^{m} q_k^-\, r_{n-k} \equiv 0 \;\Rightarrow \sum_{k=1}^{m} q_k^-\, r_{n-k} \equiv -r_n\,,\ m+1 \le n \le 2m\,. \quad (21)$$

  This forms a system of m linear equations which determines the m coefficients $(q_k^-)_{1\le k\le m}$ of the polynomial Q_-.
- **Step 1-b** This being done, projecting Eq. (19) onto the monomial basis $(1,\ldots,z^m)$ and using $Q_+(0) = 1$, the $m+1$ coefficients of the polynomial Q_+ are given by

$$q_0^+ = 1 \text{ and } q_n^+ = \sum_{k=0}^{n} q_k^-\, r_{n-k}\,,\ 1 \le n \le m\,. \quad (22)$$

In some particular cases where the specified multipole expansion exhibits certain kind of symmetries, as for instance in the case of a pure $2p$-pole magnet, the step 1-a needed to determine the polynomial Q_- could be dropped and the overall method somewhat simplified. Indeed, as it will be shown in section 3.2, if the multipole field expansion is requested to be purely $2p$-polar up to the order $2m$, the polynomials Q_- and Q_+ will be found to be linked by the following relation:

$$Q_-(z) = Q_+(e^{i\pi/p} z)\,. \tag{23}$$

The above relation implies in particular that each root $(z_k^+)_{1\leq k\leq m}$ of the polynomial Q_+, that is each wire of positive current, can be associated to a wire of opposite polarity by a simple rotation of π/p, which is a well-known feature, for instance for the standard bi-polar current dipole or quadrupole magnets.
As a more quantitative example, if the problem is to determine the positions of $2m = 14$ wires to help in the design of a 14-block magnet producing a pure dipole field ($p = 1$) up to the order $2m + 1 = 15$, we will have to solve the following polynomial equation:

$$Q_+(z) = e^z\, Q_+(-z) + \mathrm{O}(z^{15}) \text{ with } \deg(Q_+) = m = 7 \text{ and } Q_+(0) = 1\,, \tag{24}$$

the solution of which is given by

$$Q_+(z) = 1 + \frac{1}{2}\,z + \frac{3}{26}\,z^2 + \frac{5}{312}\,z^3 + \frac{5}{3432}\,z^4 + \frac{1}{11440}\,z^5 + \frac{1}{308880}\,z^6 + \frac{1}{17297280}\,z^7\,. \tag{25}$$

The 7 complex roots of this polynomial (one real and 3 pairs of complex conjugates) correspond to the position of the 7 wires with positive current, while the 7 wires of opposite polarity are obtained by applying the symmetry $z \longrightarrow -z$ (see Fig. 3(a)).

Case $P = 2$. In this paragraph, the multipole field expansion is specified up to the order M at two locations $Z_1 = -Z_2 \equiv a$ of the transverse plane. The corresponding harmonics are noted $(C_k^{(1,2)})_{1\leq k\leq M}$. The total number of wires considered is then equal to $2M$, M with a positive current and the other half with the opposite polarity. According to the relation (18), the problem is to find two polynomials $Q_\pm$ of degree $N = M$ such that

$$\left\{\begin{array}{rcl} Q_+(z+a) & \equiv & \lambda_1 Q_-(z+a) \times R_1(z) + \mathrm{O}(z^{M+1}) \\ Q_+(z-a) & \equiv & \lambda_2 Q_-(z-a) \times R_2(z) + \mathrm{O}(z^{M+1})\,, \end{array}\right. \tag{26}$$

where $\lambda_{1,2}$ are two complex numbers which do no need to be further specified[1)] and $R_{1,2}(z)$ are the polynomials of degree M defined by

$$R_{1,2}(z) \overset{\text{Eq.(9)}}{=} \exp\left[\sum_{k=1}^{M} \frac{C_k^{(1,2)}}{k}\, z^k\right] + \mathrm{O}(z^{M+1}) = 1 + \sum_{k=1}^{M} \frac{C_k^{(1,2)}}{k}\, z^k + \ldots \overset{\text{def}}{=} 1 + \sum_{n=1}^{M} r_n^{(1,2)}\, z^n\,. \tag{27}$$

In order to solve our problem, we must first introduce certain additional algebraic objects. First, we consider the Toeplitz operators $\mathcal{A}_{R_1,R_2}$ corresponding to the map of multiplication by the polynomials $R_{1,2}$ in the ring $\mathsf{C}[z]$ of polynomials in the variable z with coefficients from the complex field C:

$$\begin{array}{rccc} \mathcal{A}_{R_1,R_2}: & \mathsf{C}[z] & \longrightarrow & \mathsf{C}[z] \\ & Q(z) & \mapsto & R_{1,2}(z)\, Q(z)\,. \end{array} \tag{28}$$

[1)] With $R_{1,2}(0) \equiv 1$, and assuming that the polynomials $Q_\pm$ are solutions of Eq. (26), we have de facto $\lambda_{1,2} \equiv Q_+(\pm a)/Q_-(\pm a)$.

The matrices $A_{1,2}$ associated to these maps, when projected onto the $M+1$-dimensional vector space $\mathsf{C}_M[z]$ of the polynomials of degree equal or lower than M is the $(M+1)\times(M+1)$ lower triangular matrix given by

$$A_{1,2} = \begin{pmatrix} 1 & 0 & \dots & 0 \\ r_1^{(1,2)} & 1 & \ddots & \vdots \\ \vdots & \vdots & \ddots & \vdots \\ r_M^{(1,2)} & r_{M-1}^{(1,2)} & \dots & 1 \end{pmatrix} \tag{29}$$

In particular, the matrices $A_{1,2}$ are regular since their diagonal elements are all equal to unity. Then, for an arbitrary complex number a, we introduce the linear operator of translation $\mathcal{T}_a$ acting in the vector space $\mathsf{C}_M[z]$ of the polynomials of degree equal or lower than M:

$$\begin{array}{rccc} \mathcal{T}_a: & \mathsf{C}_M[z] & \longrightarrow & \mathsf{C}_M[z] \\ & Q(z) & \mapsto & Q(z+a)\,. \end{array} \tag{30}$$

In the usual monomial basis $(1,\dots,z^M)$, its matrix T_a is upper triangular and given by:

$$\left\{ \begin{array}{rcll} (T_a)_{i,j} & = & 0 & \text{if } 0 \le i < j \le M \\ (T_a)_{i,j} & = & \dfrac{j!}{i!(j-i)!}\, a^{j-i} & \text{otherwise}\,. \end{array} \right. \tag{31}$$

For two arbitrary complex numbers a and b, it is easy to see that the associated translation matrices $T_{a,b}$ commute each other and concatenate as follows:

$$T_a\, T_b = T_b\, T_a = T_{a+b}\,. \tag{32}$$

In particular, the matrix T_a is regular with an inverse equal to T_{-a}.
Finally, depending on the context, we will continue using the notations $Q_\pm$ either to refer to the polynomials themselves or to the associated $(M+1)$-dimensional vectors after projection onto the usual basis $(1,\dots,z^M)$, i.e.:

$$Q_\pm \equiv \begin{pmatrix} q_0^\pm \equiv 1 \\ q_1^\pm \\ \vdots \\ q_M^\pm \end{pmatrix}\,. \tag{33}$$

With all these new notations, the equation (26) can then be re-expressed as follows:

$$\left\{ \begin{array}{rcl} T_a\, Q_+ & \equiv & \lambda_1\, A_1\, T_a\, Q_- \\ T_{-a}\, Q_+ & \equiv & \lambda_2\, A_2\, T_{-a}\, Q_- \end{array} \right. \tag{34}$$

After some algebra and using the properties of the matrices $A_{1,2}$ and T_a, the above equation leads to

$$\left[\underbrace{T_{-a}\, A_1\, T_a^2\, A_2^{-1}\, T_{-a}}_{\stackrel{\text{def}}{=} A} \right] Q_+ = \lambda\, Q_+ \text{ with } \lambda \stackrel{\text{def}}{=} \lambda_2/\lambda_1\,. \tag{35}$$

In other words, the vector Q_+ is an eigen vector for the matrix A defined above which, in addition, has to be normalised using the condition $Q_+(0) = q_0^\pm \equiv 1$. Then, using one of the two

relations given in Eq. (34), the vector Q_- can be determined within a multiplicative constant, which is further evaluated using the condition $Q_-(0) = q_0^- \equiv 1$.
One very interesting aspect is that the matrix A of dimension $M+1$ generally possess $M+1$ distinct eigenvalues associated to $M+1$ possible polynomials Q_+ which are de facto linearly independent. In other words, this means $M+1$ possible choices of a priori completely different topological nature for the positioning of the $2M$ wires. This discussion will be continued on a more quantitative basis in section 4.1 when dealing with the so-called "sextupole-like quadrupole". In particular, we will show on a specific example that in general only one of the $M+1$ eigen-polynomials do not possess any roots in the magnet mid-plane, but without being able to bring any general proof of this result.

2.4 Magnetic potential and generating function

Before going to practical applications, a small digression could be inserted in the text to discuss the physical interpretation of the generating function $\mathcal{G}$ introduced in Eq. (5).
Let us consider a convex region of the transverse plane which is free of wires, say the magnet aperture centered around $z = 0$. In this area the function $\mathcal{G}(z)$ does not vanish by construction. We can therefore consider its complex logarithm defined by

$$\log\left[\mathcal{G}(z)\right] \equiv \underbrace{\log\left|\mathcal{G}(z)\right|}_{\stackrel{\text{def}}{=} A_s(x,y)} + i\,\underbrace{\arg\left[\mathcal{G}(z)\right]}_{\stackrel{\text{def}}{=} \phi(x,y)}\,. \tag{36}$$

As real and imaginary parts of an holomorphic function, the real functions $A_s(x,y)$ and $\phi(x,y)$ defined above fulfill the Cauchy-Riemann equations:

$$\left\{\begin{array}{rcl} \partial_x A_s &=& \partial_y \phi \\ \partial_y A_s &=& -\partial_x \phi\,. \end{array}\right. \tag{37}$$

Therefore, we have

$$\begin{array}{rcl} \left(\partial_x - i\partial_y\right) A_s &=& \left(\partial_y + i\partial_x\right)\phi \\ &=& \dfrac{1}{2}\left(\partial_x - i\partial_y\right)\left(A_s + i\phi\right) \\ &=& \partial_z \log[\mathcal{G}] = \dfrac{\mathcal{G}'}{\mathcal{G}} \stackrel{\text{Eq. (5)}}{=} B_y + i\,B_x\,. \end{array} \tag{38}$$

In other words, the functions A_s and ϕ can be interpreted as the longitudinal vector potential and the scalar potential associated to the 2D magnetic field induced by the N wires of current I_n:

$$\left[B_x,\, B_y\right] = \mathrm{grad}\phi = -\mathrm{Curl}\left[A_s\,\mathbf{e}_s\right] \tag{39}$$

In particular, the field lines are given by the conditions

$$A_s(x,y) = \log\left|\mathcal{G}(x+iy)\right| = \mathbf{Cst} \;\Rightarrow \left|\mathcal{G}(z)\right| = \mathbf{Cst}\,. \tag{40}$$

3 Distribution of wires associated to a given truncated multipole expansion of the field at one single location of the transverse plane

This section will present several applications of the methods in the case $P = 1$, that is the determination of the position of M wires to generate a given 2D magnetic field for which the multipole expansion up to the order M is specified at one single position of the transverse plane. In the first two sub-sections, dealing with unipolar-current and bipolar-current configurations,

we will present the case of pure $2N$-pole magnets, that is a 2D magnetic field for which all the harmonics C_k but one, the harmonics $C_N \equiv 1$, are null up to the order M. Then the example of a dipole-quadrupole combined magnet will be illustrated in sub-section 3.3. In the last two sub-sections, the unipolar and bipolar-current configurations will be qualitatively compared in terms of geometry, aperture and field quality, and also briefly in terms of efficiencies, that is gauss/ampere or $B_{\rm peak}/B(z=0)$. In addition, different possible strategies for stacking several layers of wires will be discussed in order to reach the magnetic field or magnetic gradient required at the center of the aperture, while preserving or even improving the purity of the field produced.

3.1 Pure $2N$-pole magnet approximated with an unipolar-current wire distribution

We start with the most simple configuration where all the current I_n are set to unity (unipolar-current magnets). The multipole expansion of the magnetic field is specified at one single location of the transverse plane, $Z = 0$, and supposed to approach an unit dipole up to the order M:

$$C_1 \equiv 1 \text{ and } C_k \equiv 0\,,\ 2 \leq k \leq M\,. \tag{41}$$

Following Eq.'s (9) and (13), the position of M wires are simply given by the M complex roots of the following polynomial:

$$\mathcal{G}(z) \equiv Q_+^{\rm dip}(z) = \underbrace{Q_+^{\rm dip}(0)}_{\equiv 1} \times \exp(z) + \mathrm{O}(z^{M+1}) = \sum_{k=0}^{M} \frac{z^k}{k!}\,. \tag{42}$$

The "unipolar-current" dipole corresponding to $M = 14$ wires is shown in Fig. 1(a), where all the harmonics strictly below C_{15} have been eliminated. In the case where the multipole field expansion is assumed to be purely $2N-$polar up to the order $N \times M$, $N > 1$, the generalization is straightforward. The position of the $M \times N$ wires is indeed given by the complex root of the polynomial

$$\mathcal{G}(z) \equiv Q_+^{\rm 2N-pole}(z) = \exp(z^N/N) + \mathrm{O}(z^{NM+1}) = \sum_{k=0}^{M} \frac{z^{Nk}}{N^k k!} \equiv Q_+^{\rm dip}(z^N/N)\,. \tag{43}$$

More simply, for each of the M roots $(z_m^{\rm dip})_{1\leq m\leq M}$ of the polynomial $Q_+^{\rm dip}$, it is sufficient to calculate the N complex numbers corresponding to one of the $N^{\rm th}$ roots of $N\times z_m^{\rm dip}$. In this way we obtain directly a very pure $2N$-pole with $C_N = 1$ and for which all the other harmonics of order strictly lower than $N \times M + 1$ have been eliminated[2)]. The corresponding quadrupole, sextupole and octupole made of $2\times 14 = 28$, $3\times 14 = 42$ and $4\times 14 = 56$ wires are showed in Fig. 1 for the field lines, and Fig. 2, for the contours of constant field magnitude errors w.r.t. the ideal $2N$-pole field (i.e. $\left|\mathbf{B}(z) - z^{N-1}\right|$).

3.2 Pure $2N$-pole magnet approximated with a bipolar-current distribution

As previously, we start with the case of a magnetic field which is specified to be purely dipolar up to the order M with $C_1 \equiv 1$, M being assumed to be an even integer in this case. Following Eq.'s (9) and (18), the location of $M/2$ wires of positive and negative currents are

[2)] For symmetry reasons, all the harmonics strictly lower than $N \times (M+1)$ are in fact eliminated in this case with only $N \times M$ wires.

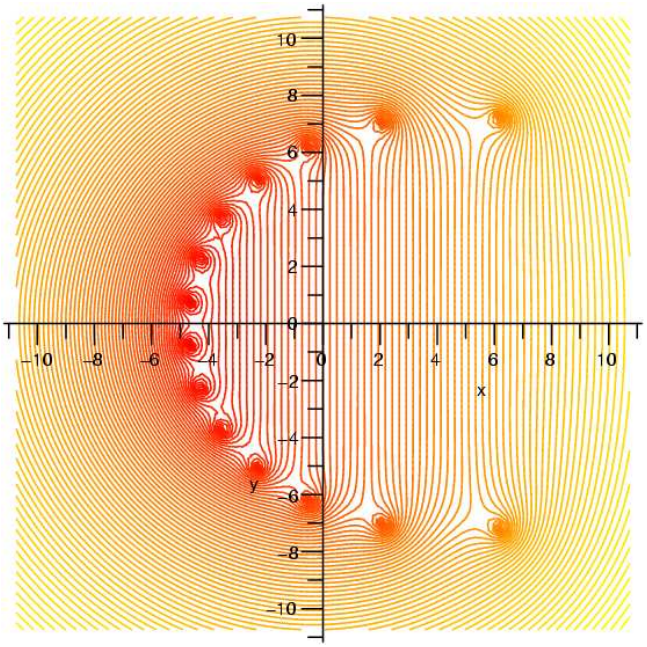

(a): Unipolar-current dipole

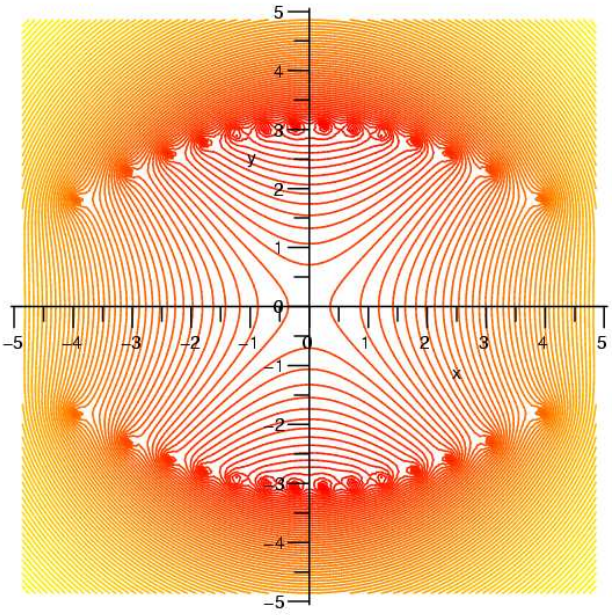

(b): Unipolar-current quadrupole

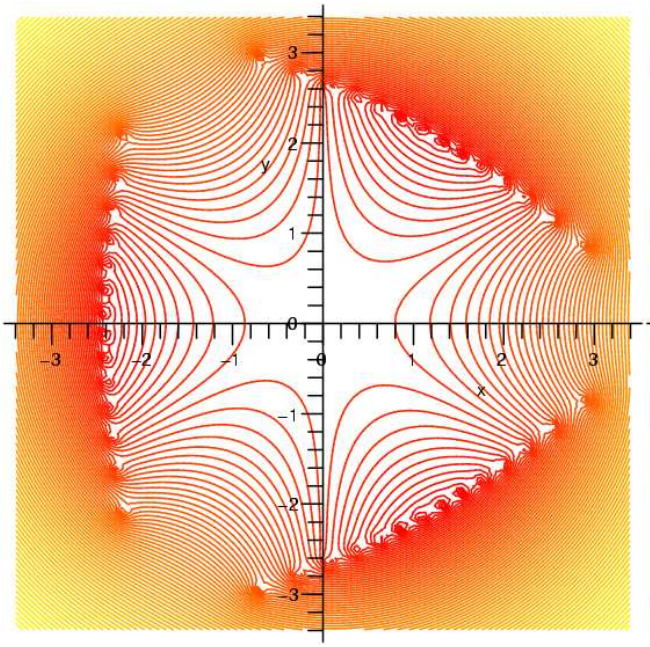

(c): Unipolar-current sextupole

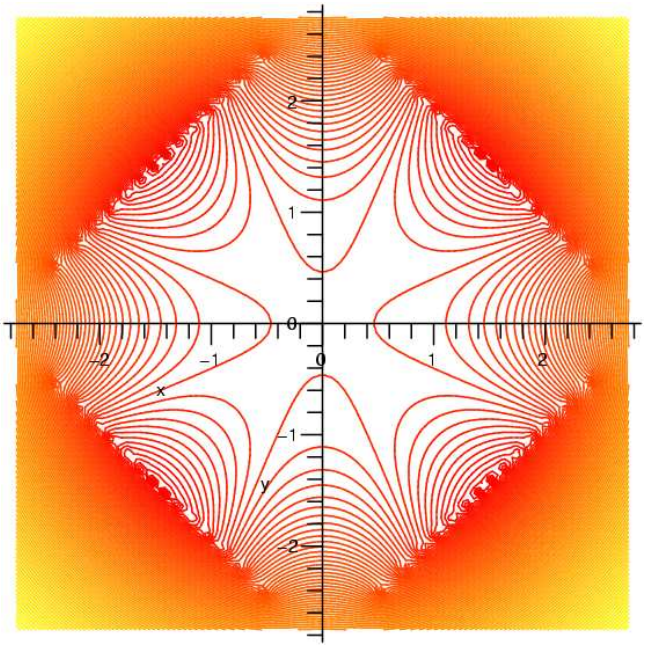

(d): Unipolar-current octupole

Figure 1: Field lines for the unipolar-current dipole, quadrupole, sextupole and octupole magnets made of 14, 28, 42 and 56 wires, respectively.

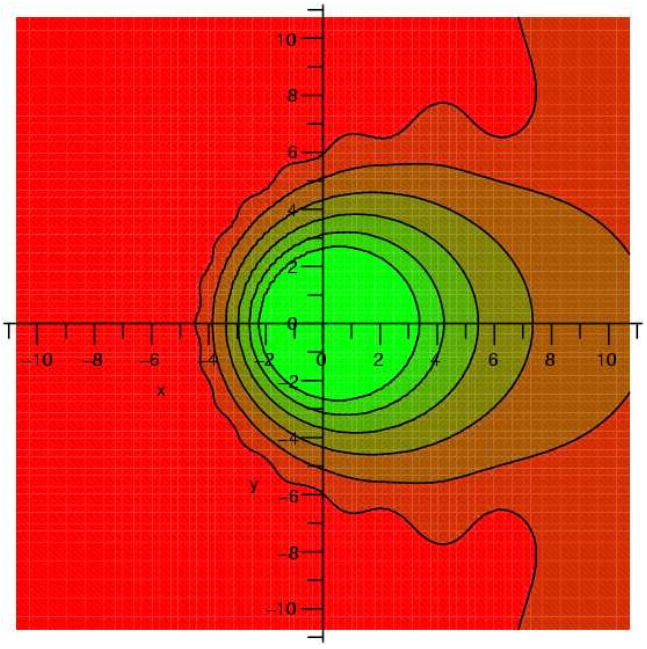

(a): Unipolar-current dipole

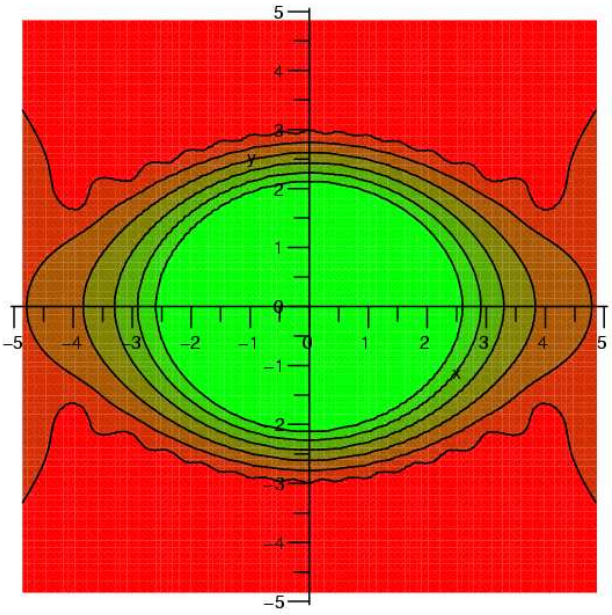

(b): Unipolar-current quadrupole

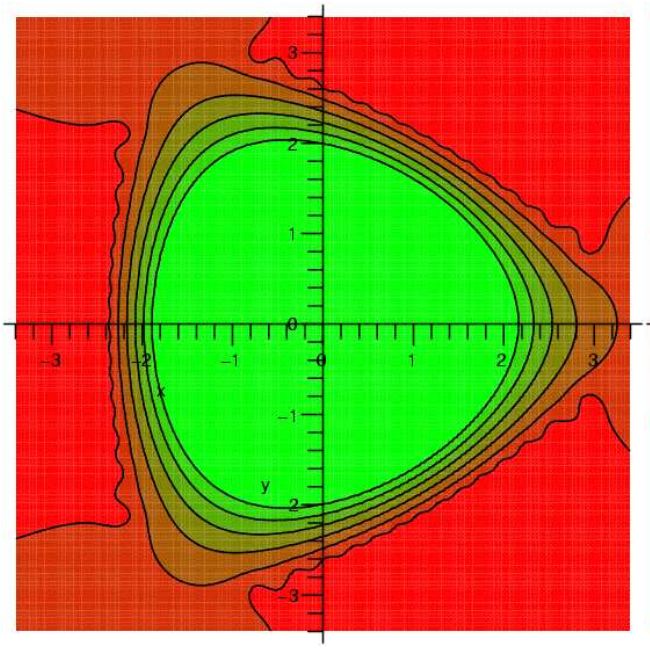

(c): Unipolar-current sextupole

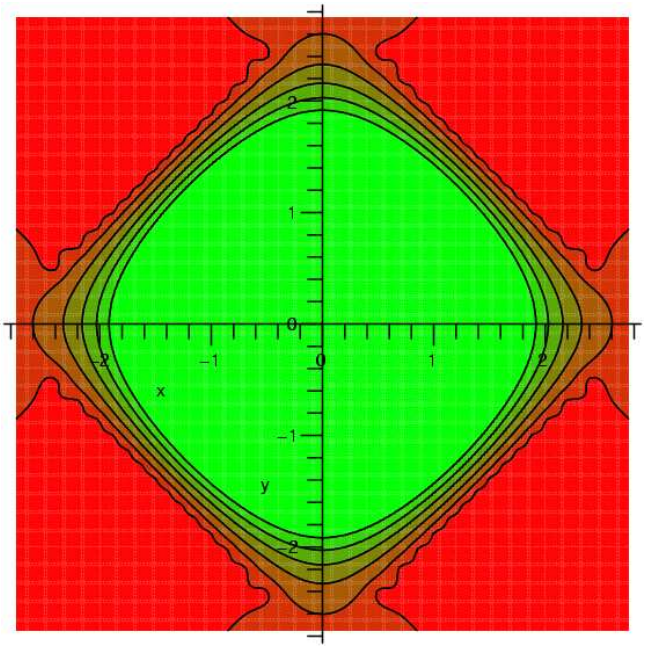

(d): Unipolar-current octupole

Figure 2: Contours of constant field magnitude error w.r.t. the ideal $2N$-pole magnetic field (i.e. the quantity $\left|\mathbf{B}(z) - z^{N-1}\right|, N = 1, \ldots, 4$) for the unipolar-current dipole, quadrupole, sextupole and octupole magnets made of 14, 28, 42 and 56 wires, respectively: the six levels indicated correspond to relative field errors less than 0.1 unit of 10^{-4} (10 ppm), 1 unit, 10 units, 1%, 10% and 100%.

given by the complex roots of the two polynomials $Q_\pm$ of degree $M/2$, satisfying $Q_\pm(0) = 1$ and which fulfill the following functional relation:

$$Q_+^{\rm dip}(z) = \exp(z)\, Q_-^{\rm dip}(z) + {\rm O}(z^{M+1})\,. \tag{44}$$

As showed in Eq.'s (21) and (22), this relation is equivalent to two linear systems in the coefficients of $Q_\pm$, which then can be solved numerically to determine in an unique way these two polynomials.
This being said and as previously announced, one can push a bit further the analytical treatment of this specific case. Indeed, by considering the above relation for z and $-z$ and by multiplying the two corresponding equalities, one gets

$$Q_+^{\rm dip}(z)\, Q_+^{\rm dip}(-z) = Q_-^{\rm dip}(z)\, Q_-^{\rm dip}(-z) + {\rm O}(z^{M+1})\,. \tag{45}$$

The polynomials occurring on both sides of this relation are of degree $2\times M/2 = M$. Therefore the above relation is in fact a strict equality:

$$Q_+^{\rm dip}(z)\, Q_+^{\rm dip}(-z) = Q_-^{\rm dip}(z)\, Q_-^{\rm dip}(-z)\,. \tag{46}$$

Therefore, this implies that the polynomial $Q_-^{\rm dip}(z)$ divides the polynomial $Q_+^{\rm dip}(z)\times Q_+^{\rm dip}(-z)$. Then, remembering that the polynomials Q_- and Q_+ are coprime (see the discussion leading to Eq. (17)), we conclude easily that the initial condition (44) is in fact equivalent to

$$\left\{\begin{array}{rcl} Q_-^{\rm dip}(z) & \equiv & Q_+^{\rm dip}(-z) \\ Q_+^{\rm dip}(z) & = & \exp(z)\, Q_+^{\rm dip}(-z) + {\rm O}(z^{M+1}) \text{ with } \deg(Q_+^{\rm dip}) = M/2 \text{ and } Q_+^{\rm dip}(0) = 1\,. \end{array}\right. \tag{47}$$

Finally, as in the unipolar configuration, it is easy to see that the general case of the pure $2N$-pole (up to the order $N\times M$) can be deduced from the dipolar case by using the following relations:

$$Q_\pm^{\rm 2N-pole}(z) = Q_\pm^{\rm dip}(z^N/N) \Rightarrow Q_-^{\rm 2N-pole}(z) \stackrel{\rm Eq.(47)}{=} Q_+^{\rm dip}(-z^N/N) = Q_+^{\rm 2N-pole}\left(e^{i\pi/N} z\right)\,. \tag{48}$$

The polynomials $Q_+^{\rm dip}$ of degree $1,\,\ldots,\,7$ which satisfy the relation (47) for $M = 2,\,4,\,\ldots,\,14$ are given below

$$\begin{array}{ll}
Q_+^{\rm dip}{=}1 + \frac{z}{2} & \text{for } M = 2 \\
Q_+^{\rm dip}{=}1 + \frac{z}{2} + \frac{1}{12}\, z^2 & \text{for } M = 4 \\
Q_+^{\rm dip}{=}1 + \frac{z}{2} + \frac{1}{10}\, z^2 + \frac{1}{120}\, z^3 & \text{for } M = 6 \\
Q_+^{\rm dip}{=}1 + \frac{z}{2} + \frac{3}{28}\, z^2 + \frac{1}{84}\, z^3 + \frac{1}{1680}\, z^4 & \text{for } M = 8 \\
Q_+^{\rm dip}{=}1 + \frac{z}{2} + \frac{1}{9}\, z^2 + \frac{1}{72}\, z^3 + \frac{1}{1008}\, z^4 + \frac{1}{30240}\, z^5 & \text{for } M = 10 \\
Q_+^{\rm dip}{=}1 + \frac{z}{2} + \frac{5}{44}\, z^2 + \frac{1}{66}\, z^3 + \frac{1}{792}\, z^4 + \frac{1}{15840}\, z^5 + \frac{1}{665280}\, z^6 & \text{for } M = 12 \\
Q_+^{\rm dip}{=}1 + \frac{z}{2} + \frac{3}{26}\, z^2 + \frac{5}{312}\, z^3 + \frac{5}{3432}\, z^4 + \frac{1}{11440}\, z^5 + \frac{1}{308880}\, z^6 + \frac{1}{17297280}\, z^7 & \text{for } M = 14\,.
\end{array} \tag{49}$$

The bipolar-current dipole, quadrupole, sextupole and octupole magnet corresponding to $M = 14$, that is made of 14, $2{\times}14 = 28$, $3{\times}14 = 42$ and $4{\times}14 = 56$ wires, respectively, are illustrated in Fig.'s 3 and 4 for the field lines and the quality of the field produced.

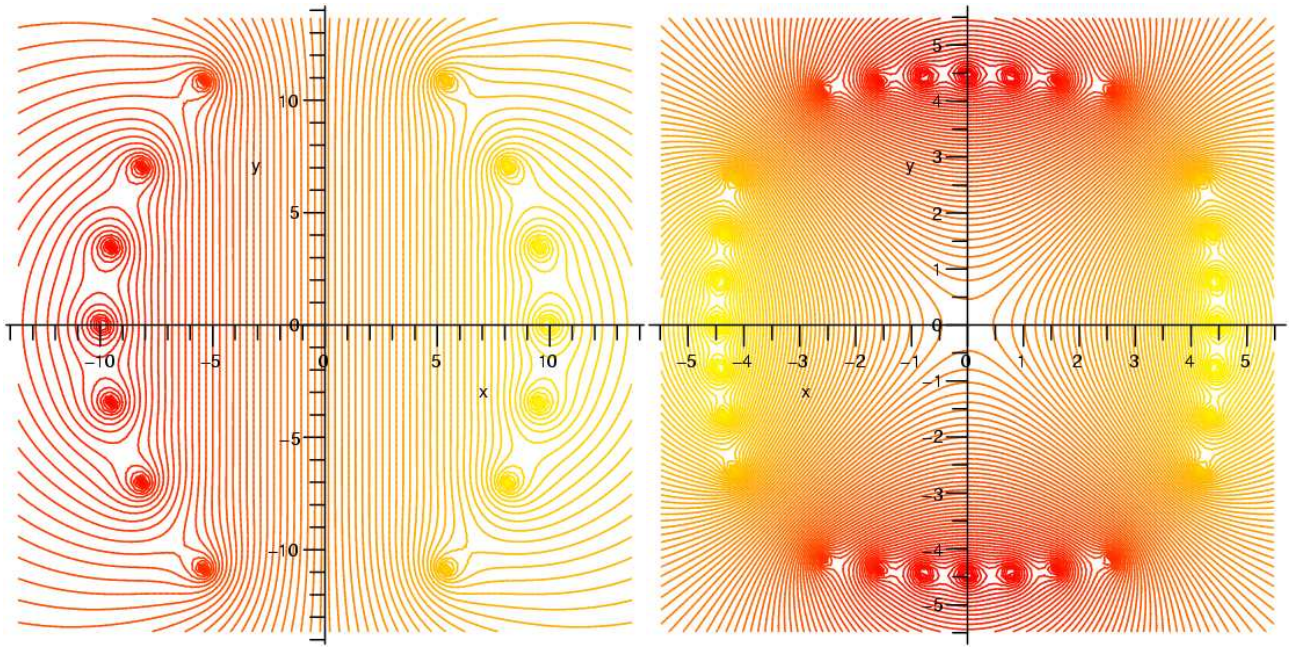

(a): Bipolar-current dipole

(b): Bipolar-current quadrupole

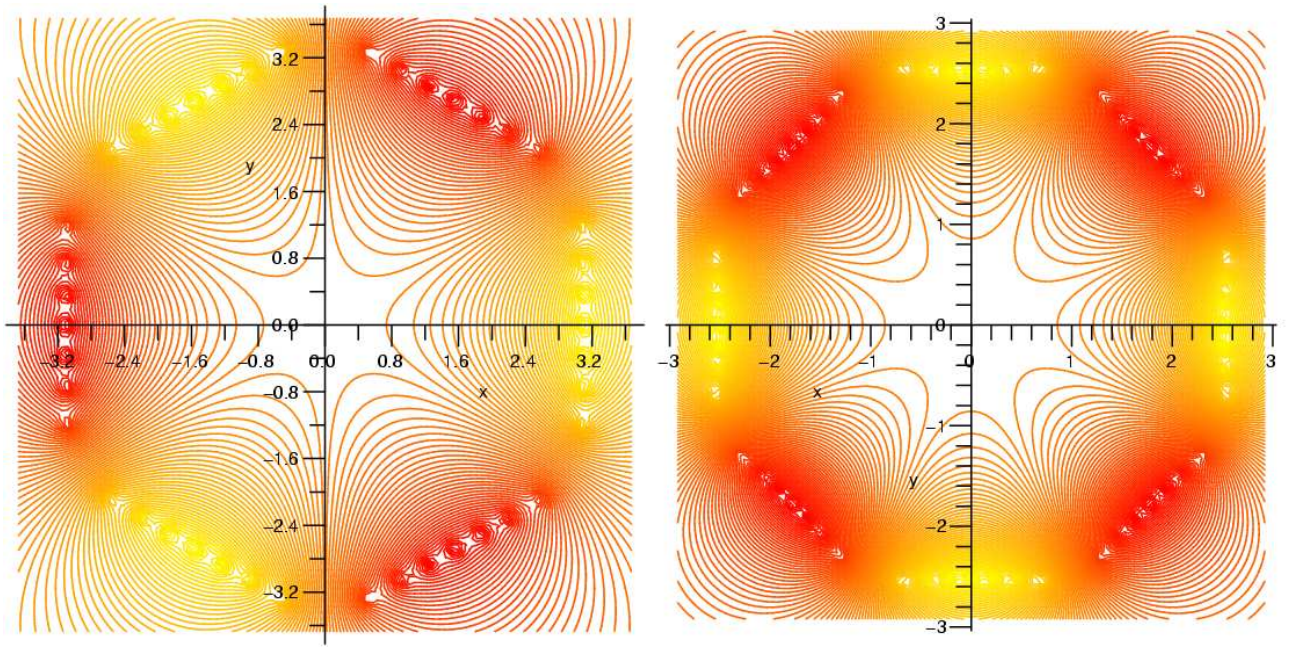

(c): Bipolar-current sextupole

(d): Bipolar-current octupole

Figure 3: Field lines of the bipolar-current dipole, quadrupole, sextupole and octupole magnets made of 14, 28, 42 and 56 wires, respectively. The yellow and red zones are in the vicinity the wires of positive and negative current, respectively.

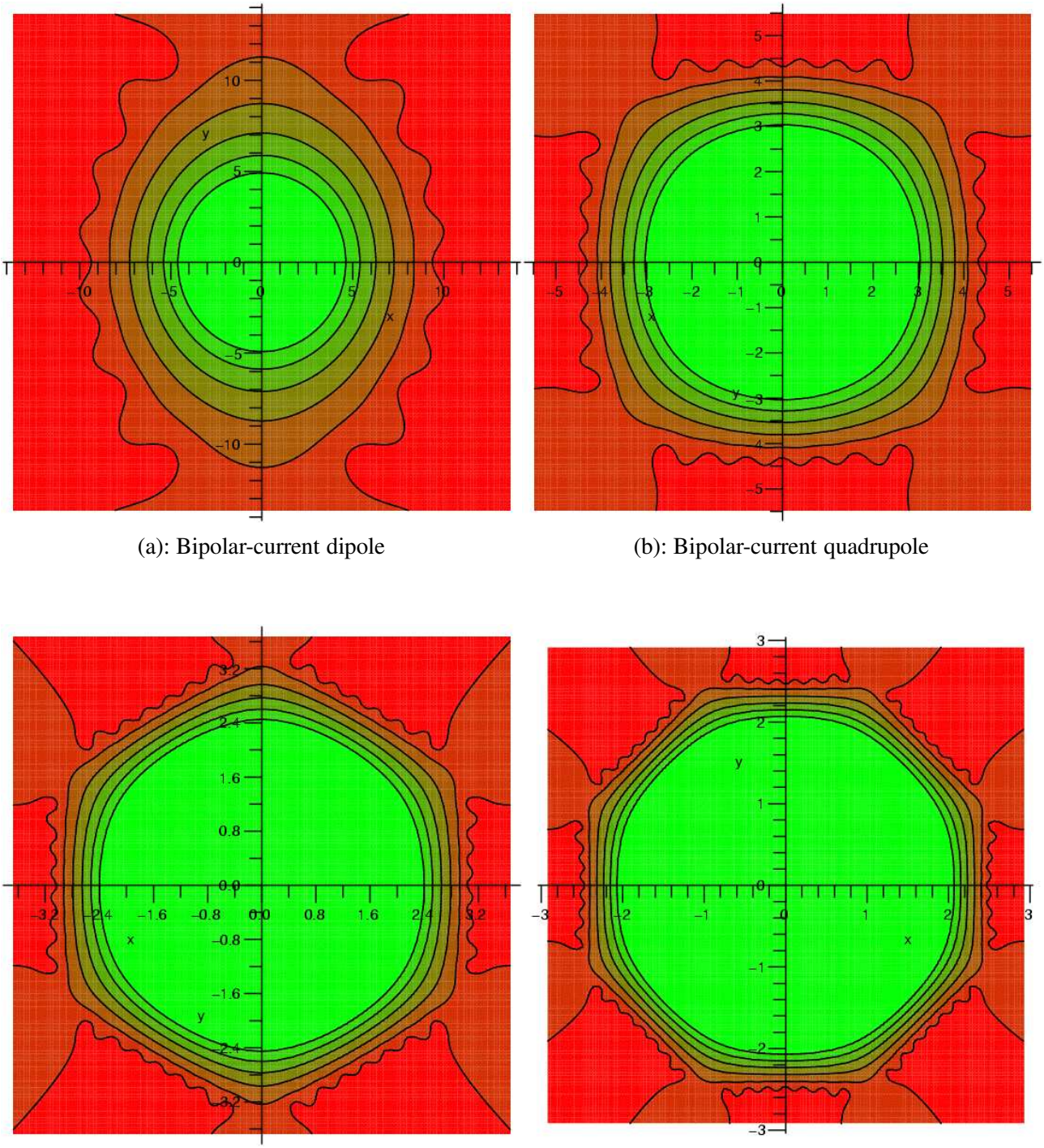

(a): Bipolar-current dipole

(b): Bipolar-current quadrupole

(c): Bipolar-current sextupole

(d): Bipolar-current octupole

Figure 4: Contours of constant field magnitude error w.r.t. the ideal $2N$-pole magnetic field (i.e. the quantity $\left|\mathbf{B}(z) - z^{N-1}\right|, N = 1, \ldots, 4$) for the bipolar-current dipole, quadrupole, sextupole and octupole magnets made of 14, 28, 42 and 56 wires, respectively: the six levels indicated correspond to relative field errors less than 0.1 unit of 10^{-4} (10 ppm), 1 unit, 10 units, 1%, 10% and 100%.

3.3 Dipole-quadrupole combined magnet and connection with FFAG magnets

In this paragraph, the method is applied to the design of a combined dipole-quadrupole magnet. As an example, the position of $N = 20$ wires is determined to produce a magnetic field for which the multipole harmonics C_k at $z = 0$ are specified as follows:

$$C_1 \equiv 5\,,\ C_2 \equiv 1 \text{ and } C_k \equiv 0\,,\ 3 \leq k \leq 20\,. \tag{50}$$

Following the techniques developed previously for an unipolar-current magnet (see section-2.3.1), the wire position is determined by finding the $N = 20$ roots of the following polynomial of degree $N = 20$:

$$Q_+(z) = \exp(5z + z^2/2) + \mathbf{O}(z^{21}) \overset{\text{Eq.(9)}}{=} \sum_{n=0}^{20} \left[\sum_{i,j,i+2j=n} \frac{5^i}{2^j\, i!\, j!} \right] z^n\,. \tag{51}$$

In the bipolar-current configuration, the positions of the 10+10 wires with positive and negative currents correspond to the roots of the two polynomials Q_+ and Q_- which are univocally determined by the following condition (see section 2.3.2):

$$Q_+(z) = \exp(5z + z^2/2)\, Q_-(z) + \mathbf{O}(z^{21}) \text{ with } \deg(Q_\pm) = 10 \text{ and } Q_\pm(0) = 1\,. \tag{52}$$

The corresponding unipolar-current and bipolar-current 20-wire magnets are showed in Fig. 5, where the field lines and contours of constant field magnitude are drawn for both configurations. It is worth mentioning the possible connection with FFAG accelerators which require a magnetic field of the form

$$\mathbf{B}(z) = B_0 \left(1 + \frac{z}{R_0}\right)^k\,, \tag{53}$$

where R_0 is the distance between the center of the ring and the magnet center $z = 0$, B_0 denotes the reference vertical dipole field of the accelerator at the reference radius $r = R_0$ and k is the so-called geometrical field index of the FFAG accelerator. In the present case, we then have $k \equiv 1$, $R_0 = C_1/C_2 = 5$ m and $B_0 = \mu_0\, I/(2\pi) \times C_1 = 10$ Gauss assuming a current of ± 1000 A circulating in the 20 wires of the magnet. This field can of course be further amplified by stacking several layers of wires (see sub-section 3.5.1 and Fig. 6(b)). However what is more relevant at this stage is that, in the bi-polar current configuration, we obtain directly a left/right asymmetric coil layout which is qualitatively very similar to that recently proposed for superconducting type magnets to be used in FFAG machines (see e.g. [4]).
Finally, both in the unipolar and bipolar-current configurations, it is rather clear that the method used can be quickly generalized for an arbitrary field index k for which the generating polynomials $Q_\pm$ can be found by solving the following functional relation:

$$\begin{cases} Q_+(z) = \exp\left[\displaystyle\int_0^z dz'\, \mathbf{B}(z')\right] + \mathbf{O}(z^{M+1}) = \exp\left[\dfrac{B_0\left((1+z/R_0)^{k+1} - 1\right)}{R_0\,(k+1)}\right] + \mathbf{O}(z^{M+1}) \\ \qquad \text{for the unipolar systems}\,, \\ Q_+(z) = \exp\left[\dfrac{B_0\left((1+z/R_0)^{k+1} - 1\right)}{R_0\,(k+1)}\right]\, Q_-(z) + \mathbf{O}(z^{M+1}) \\ \qquad \text{for bipolar systems}\,. \end{cases} \tag{54}$$

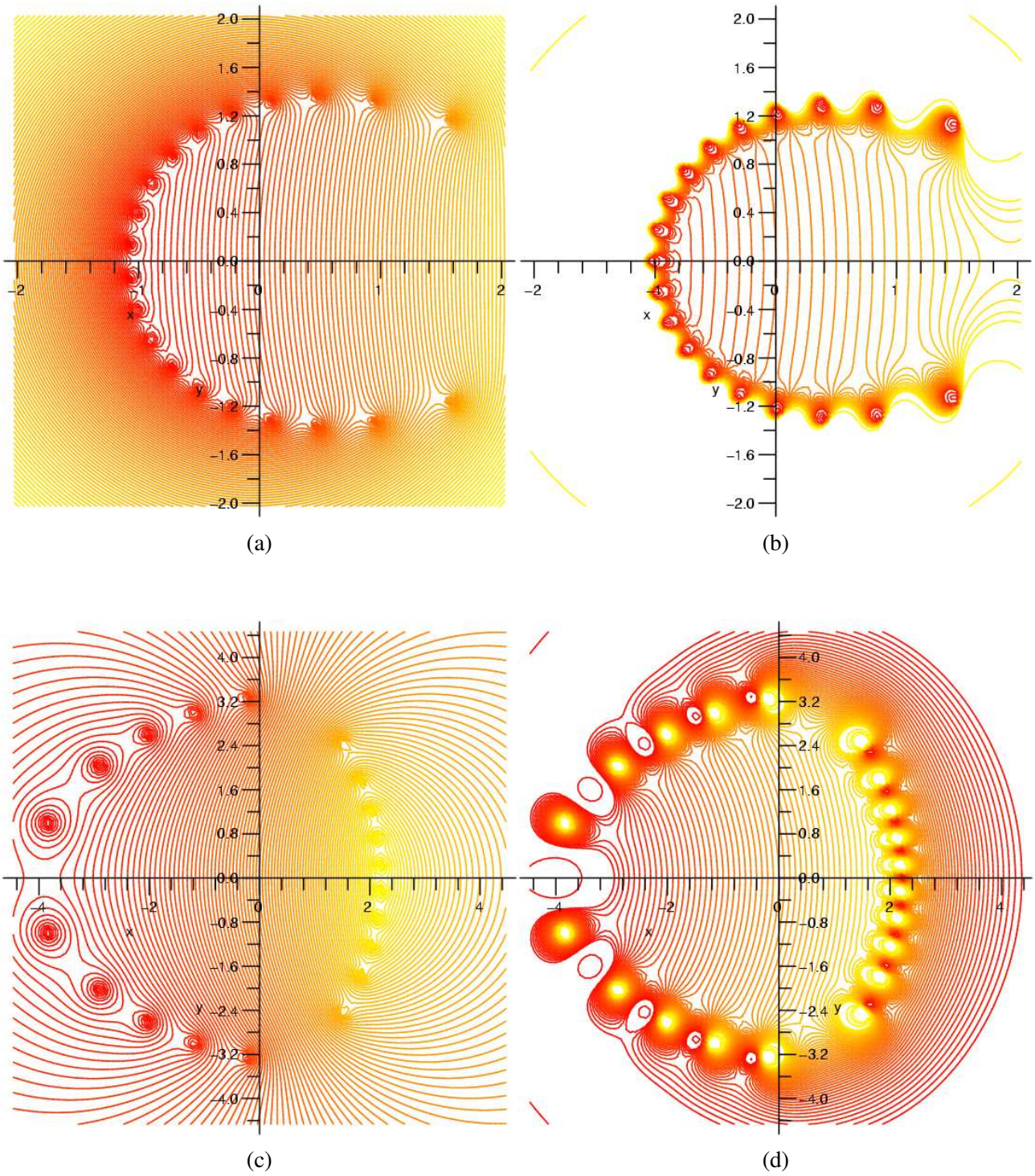

Figure 5: 20-wires unipolar-current (top) and bipolar-current (bottom) dipole-quadrupole combined magnet (with $C_1 = 5$, $C_2 = 1$ and $C_k = 0$, $3 \leq k \leq 20$). Field lines (Fig.'s (a) and (c)) and contours of constant field magnitude $\mathbf{B}$ (Fig.'s (b) and (d)).

3.4 Comparison between unipolar and bipolar-current magnets

No attempt will be made here for a thorough comparison between unipolar-current and bipolar-current magnets. However some general features are worth mentioning.

3.4.1 Coil geometry

First of all, as shown by the previous examples, it is clear that the two configurations of current studied so far (amongst many other possible ones) leads to drastically different magnet geometries. The cases of the unipolar-current dipole and quadrupole (see Fig.'s 1(a) and 1(b)) are particularly interesting due to the sizable wire-free area, respectively on the right side and on the two sides of the magnet. If applicable, these open sides in the horizontal plane leave therefore the possibility of accessing to the magnet interior or, which might be of great interest, to absorb or extract the synchrotron radiation in the case of high intensity electron storage rings (idem for the debris, if produced in one specific plane only, at the interaction point of a collider). However the price to pay is that current return paths will be a priori longer for the unipolar-current magnets, where presumably return bus-bars will be positioned outside a shield, rather than contributing for the magnetic field itself as this is the case in the bipolar configuration.
Concerning the bipolar-current $2N$-pole magnets previously considered, it is also worth noting that the wires are not confined to a right circular cylinder as it is usually the case in a standard design of superconducting magnets. On the contrary, as shown in Fig 3(b), the bipolar-current quadrupole is very similar to the well-known Panofsky quadrupole made of uniform current sheets inside a square iron box. Then, the bipolar-current sextupole and octupole are in some sens generalized Panofsky magnets, with an almost regular hexagonal and octogonal geometry.

3.4.2 Aperture and field quality

Because of their completely different geometries, it is rather difficult to compare a given unipolar and bipolar-current $2N$-pole magnet in terms of aperture. However, in the particular case of round beam, the magnet aperture could still be defined as the interior of the largest possible circle which does not intercept the wires (that is defined by the root $z_n^{\pm}$ of smallest modulus if one comes back to the formalism previously developed). Using this definition, it is clear that in the case of the unit dipole field, the bipolar-current configuration is roughly twice more favorable in terms of aperture (see Fig.'s 1(a) and 3(a)): $\min\left[|z_n^{\pm}|\,,\,1\leq n\leq 14\right]\,\sim\,10$ in the case of the bipolar-current unit dipole and $\min\left[|z_n^{+}|\,,\,1\leq n\leq 14\right]\,\sim\,5$ in the other configuration. Then, in the general case of the $2N$-pole magnet, this difference is less and less visible for N large and tends to unity as fast as $2^{1/N}$ (see e.g. the discussion following Eq. (43)). Concerning the area of the regions of good field quality, say where the relative field error w.r.t. to the ideal $2N$-pole field is less than one permil (corresponding to the third contour level on the Fig.'s 2 and 4), this tendency is approximately the same. In other words, this means that, in relative, the ratio between magnet aperture and zone of good field quality is roughly the same in both configurations ($\sim 70-80\%$), but noting that the uni-polar current quadrupole remains nevertheless very competitive, also in absolute, concerning the horizontal extension of the good field quality region (compare Fig.'s 2(b) and 4(b)).

3.4.3 Efficiencies

Working at constant aperture, the above discussion can also be rephrased in terms of efficiency for the generation of a magnetic field of given magnitude or of given gradient at the magnet center, assuming a given current I circulating in the wires and a given aperture of the magnet defined by a inner radius $R_{\rm in}$. More precisely, for a given $2N$-pole, one deduces

from above that the quantity $|\mathbf{B}(z=0)|\,/I/R_{\rm in}^N$ is roughly twice smaller in the case of unipolar-current magnets. For instance, rescaling to 28 mm the inner radius $R_{\rm in}$ [3)] of the 14-wire unipolar and bipolar-current dipoles showed in Fig.'s 1(a) and 3(a) and assuming a density of current j of 1000 A/mm^2 circulating in the wires, the dipole field produced at the magnet center will be around 0.04 T and 0.08 T, respectively, for a total cross-section of conductor equal to 14 mm^2. Finally, another interesting quantity concerns the ratio of this field with respect to the peak magnetic field which is reached in the magnet coils. This ratio shall be as high as possible, e.g. for super-conducting magnets operating very close to the critical surface $B_c(j)$. Without going into the details of this discussion, which is beyond the scope of this paper, we will just mention that the unipolar-current magnets are again slightly less performing with this respect.

3.5 Strategies for stacking the wires

All this brings us to the study of multi-layer magnets obtainable by different possible wire stacking strategies, in order to enhance the magnitude of the magnetic field produced, while preserving or improving its quality in the vicinity of the magnet center. In this section, the multipole expansion of the magnetic field is assumed to be specified up the order M where most of the harmonics $C_k, k \leq M$, are set to zero, with the exception of a few of them which are prescribed on purpose to non-zero values (e.g. the single component $C_N, N \leq M$ for the $2N$-pole magnets studied in sections 3.1 and 3.2 or the dipole and quadrupole components C_1 and C_2 in the case of the combined magnet described in sub-section 3.3). We define hereafter two possible strategies to build up a multi-layer magnet for which the integer M defined above will be kept constant or will vary during the layer stacking process. While each of the following strategies can in principle be applied to any of the magnet types discussed so far, we will restrict ourselves to a rather limited number of examples in order to preserve as much as possible the clarity of the discussion.

3.5.1 Radial stacking strategy at constant field quality

The most straightforward strategy is to stack different layers of wires in an homothetic way starting from a mono-layer configuration with M wires which ensures a given multipole expansion up to the order M. More precisely, let us start with a wire configuration defined by M complex numbers $(z_i)_{1\leq m\leq M}$ which are the M roots of a polynomial Q_+ of degree M (resp. of two polynomials $Q_\pm$ of degree $M/2$) satisfying a functional relation of the type:

$$\begin{aligned} Q_+(z) &= \exp\left[\sum_{k=1}^{M} C_k z^k/k\right] + \mathrm{O}(z^{M+1})\,, \ \text{ or} \\ Q_+(z) &= \exp\left[\sum_{k=1}^{M} C_k z^k/k\right] \times Q_-(z) + \mathrm{O}(z^{M+1})\,, \end{aligned} \tag{55}$$

depending on whether the magnetic system considered is of unipolar or bipolar type. For any complex number α, it is clear that the polynomials $Q_\pm(z/\alpha)$ satisfy a similar functional relation changing the harmonics C_k into C_k/α^k. More generally, let us introduce a set of L scale factors, says uniformly distributed on the positive real axis:

$$\alpha_l \equiv \alpha_0\,(1+l\delta_\alpha)\ , 1 \leq l \leq L\,, \ \text{with } \delta_\alpha \ll 1\,. \tag{56}$$

[3)] $R_{\rm in} = 28$ mm corresponds to the inner coil radius of the LHC main dipole magnets.

Based on the argument of above, it is clear that the $L \times M$ wires defined by the complex numbers $(\alpha_l z_m)$ will produce the following magnetic field around $z = 0$:

$$\mathbf{B}(z) = \sum_{k=1}^{M} \beta_k \, C_k \, z^{k-1} + \mathbf{O}(z^{M+1})$$

$$\text{with } \beta_k \stackrel{\text{def}}{=} \frac{1}{\alpha_0^k} \sum_{l=1}^{L} \frac{1}{(1 + l\,\delta_\alpha)^k} \approx \frac{1}{\alpha_0^k} \int_0^L dl \, \frac{1}{(1 + l\,\delta_\alpha)^k} \sim \begin{cases} \dfrac{1}{\delta_\alpha \, \alpha_0} \log L & \text{if } k = 1 \\ \dfrac{1}{(k-1)\,\delta_\alpha \, \alpha_0^k} & \text{otherwise.} \end{cases} \tag{57}$$

In other words, this process will not generate new non-zero harmonics, which means that the field quality is preserved, and the non-zero harmonics will be enhanced by the factors β_k.
However, while this strategy presents no intrinsic limitations to amplify the produced dipole field ($\beta_1 \propto \log(L)$ for a large number L of layers), the $2N$-pole magnets of higher order cannot be pushed to arbitrarily high gradient, assuming a given magnet aperture (related to α_0) and noting that the distance between two consecutive layers (related to δ_α) has a lower limit given by the finite dimension of the wires themselves. Furthermore, in practice, the wires will be restricted to only M azimuthal directions of the transverse plane, leaving sizable coil-free space which would be better used to contribute to the production of the required magnetic field and then maintain within reasonable bounds the radial dimensions of the magnet. Finally, considering the case of a combined magnet, that is with more than one non-zero specified harmonics, this method tends to decrease the harmonics ratios $C_k/C_1, 1 \leq k \leq N$, with no guaranty that, after the stacking process, they finally converge to their prescribed value.
In order to overcome this potential limitation, a more subtle approach consists in solving L times the functional relation (55) associated to L different set of harmonics $(C_k^{(l)})_{1 \leq l \leq L}$ on which the only constraint is that each specified harmonics C_k actually corresponds to the sum over the index l of the harmonics $C_k^{(l)}$. There is of course an infinite number of possible choices for the L sets$(C_k^{(l)})_{1 \leq l \leq L}$.
One possible choice is to see a combined magnet as the superposition of several pure $2N$-pole magnets, putting the $2N$-pole layers of the highest order as close as possible to the magnet center in order to maximize the magnet aperture at constant $2N$-polar gradient. Another possibility, more economical in terms of the total number of wires which are needed, consists in superposing on top of each other several combined magnets according to the following strategy.

- For a given harmonics of order k, the ratios $(C_k^{(l)}/C_1^{(l)})_{1 \leq l \leq L}$ are kept constant for all layers:

$$C_k^{(l)} = C_1^{(l)} \times \left(\frac{C_k}{C_1} \right)_{\text{spec.}}, 1 \leq k \leq M \,, \; 1 \leq l \leq L \,. \tag{58}$$

- The first non-zero harmonics produced by the first layer, say $C_1^{(1)}$, is numerically adjusted to match the prescribed magnet aperture (knowing that the inner aperture of the magnet obviously increases when its main field decreases).
- the set of harmonics $(C_1^{(l)})_{1 \leq l \leq L}$ is decreasing with l and is adjusted step by step such that, for instance, the minimum distance between two wires belonging to two consecutive layers is kept constant.
- the stacking process is stopped when

$$\sum_{l=1}^{L} C_1^{(l)} \approx (C_1)_{\text{spec.}} \,. \tag{59}$$

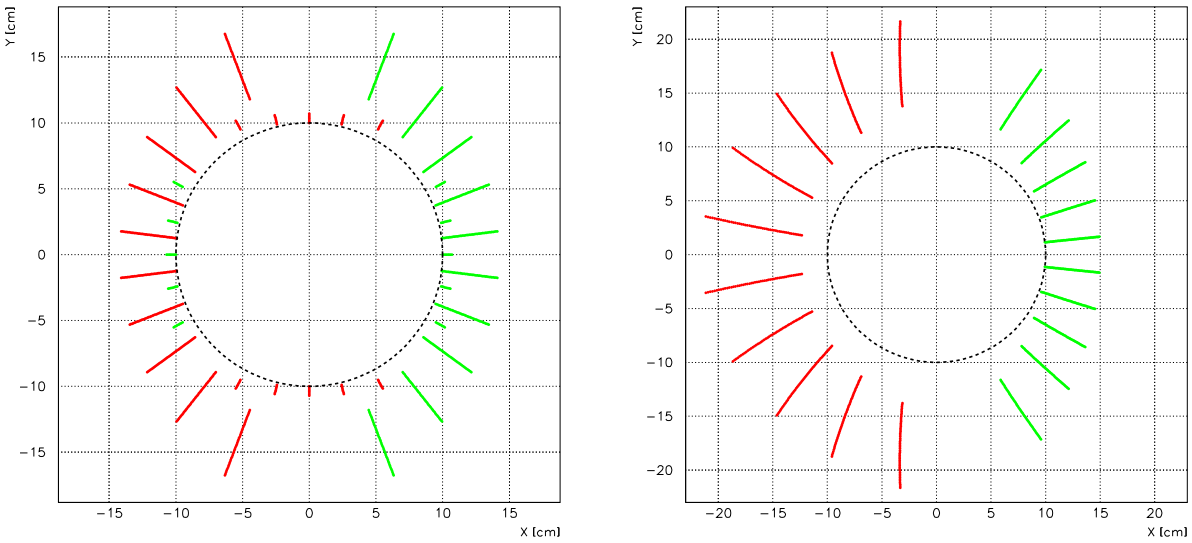

(a) (b)

Figure 6: Bipolar-current combined magnet made of 51 layers of 20 wires, with an inner aperture radius adjusted to 10 cm and producing a pure dipole-quadrupole field up to the order $M = 20$ with $C_1 = 5000$ and $C_2 = 10000$. The green and red wires are of positive and negative current, respectively. Fig. (a) has been obtained by superposing a pure 43-layers dipole (with $C_1 = 5000$) and a pure 8-layers quadrupole (with $C_2 = 10000$) while Fig. (b) is the superposition of $L = 51$ dipole-quadrupole combined magnets for which the set of harmonics $(C_1^{(l)}, C_2^{(l)})_{1 \leq l \leq L}$ fulfills the conditions enumerated in section 3.5.1.

These two possibles options are illustrated in Fig. 6 in the case of a dipole-quadrupole combined magnet (in the bipolar-current configuration), possessing an inner aperture radius of 10 cm and for which the field quality is specified up to the order $M = 20$ with $C_1 = 5000$ and $C_2 = 10000$. This corresponds to a dipole field of 1T and a quadrupole gradient of 2T/m assuming a current of $\pm$ 1000 A in the wires. In both cases, the minimum distance between two consecutive layers of wires has been kept constant, tuned to 1 mm, and the total number of layers needed has been found to be equal to $L = 51$ (more precisely, 8 quadrupole layers and 43 dipole layers in the case where the combined magnet is obtained by the strict superposition of the corresponding dipole and quadrupole). As a result, thee two configurations have also been found rather similar in terms of peak coil field, of the order of 1.5 T assuming a current of $I = 1000$ A in the wires. However, as expected by construction, the geometry of this two magnets is drastically different. In the first case, we recognize the superposition of a pure dipole magnet on top of a pure quadrupole (see Fig.'s 3(a) and 3(b)) and, for each of these two structures, the $M = 20$ corresponding azimuthal directions around which the wires are distributed. In the second case, these 20 azimuthal directions are slightly curved due to the fact that the ratios $(C_2^{(l)}/C_1^{(l)})_{1 \leq l \leq L}$ have been kept constant in the stacking process (see the short discussion after Eq. (57)). The magnet dimension is also significantly increased, which indicates in particular that the distance between two individual wires belonging to two consecutive layers can be much larger than the 1 mm minimum inter-layer distance. In others words, this means a much more difficult geometry to achieve in practice but, contrary to the first layout, a possibly better mechanical stability due to the strict separation between the wires of positive and negative current.
To summarise briefly, the radial stacking strategy appears particularly well-suited to help in the design of magnets with low or moderate gradient. Indeed, it allows to determine rapidly not

only the few azimuthal directions where the blocks of conductor have to be roughly positioned (eventually for a further numerical optimization) but it also gives a quick estimate of the radial extension of the blocks in order to ensure the production of a magnetic field of good quality with a given magnitude at the magnet center.

3.5.2 Azimuthal stacking strategy at improved field quality

As shown in the previous section, the radial stacking process allows to select only a few azimuthal directions where the wires concentrate, with, as a result, sizable coil-free spaces which would be better used to further push the magnet transfer function B/I. These M specific azimuthal directions are directly given by the order M up to which the multipole expansion of the magnetic field has been specified. Therefore, it is natural to study multi-layer magnets for which each layer of wires l, $1 \leq l \leq L$, contributes to the generation of the prescribed main field, while warranting a purity of the magnetic field up to a given oder M_l, changing with l and eventually much larger than the minimum required order M.

Without giving a rigorous proof of what follows, the tendency is that at constant main field specified up to the order M, the radial position of the M corresponding wires goes to infinity when M becomes arbitrarily large. In other words, at constant aperture, improving the field quality (by increasing the order M) is also a very efficient way to enhance the magnet transfer function, which can be physically explained by an increase of the azimuthal wire density. This effect can be easily seen in the case of the unit unipolar or bipolar-current dipole made of M wires, the transverse positions of which are given by the M or $M/2$ roots of the polynomial Q_+ fulfilling the following relations (see Sub-Sections 4.1 and 4.2):

$$\begin{aligned} Q_+(z) &= \sum_{k=0}^{M} \frac{z^k}{k!} = \exp(z) + \mathrm{O}(z^{M+1}) \text{ for the unipolar-current dipole} \\ \frac{Q_+(z)}{Q_+(-z)} &= \exp(z) + \mathrm{O}(z^{M+1}) \text{ with } \deg(Q_+) = M/2 \text{ for the bipolar-current dipole.} \end{aligned} \tag{60}$$

Since the exponential function does not admit any root in the complex plane, except at $z = -\infty$, it is rather clear that by approaching uniformly the function $\exp(z)$, that is, in particular, by increasing the degree of polynomial Q_+, its root of smallest radius will automatically move away from the origin.

As an example, Fig. 7 presents the case of a bipolar-current quadrupole magnet, with an inner radius adjusted to 5 cm and made of $L = 13$ layers of wires, each of them producing a pure quadrupolar field up to an order $(M_l)_{1\leq l\leq L}$, with $M_1 = 60$, $M_2 = 56, \ldots$, and $M_{13} = 12$, and choosing 1 mm for minimum distance between two consecutive layers. The quadrupole harmonics of this magnet has been found equal to $C_2 \approx 110'000$. This means a quadrupole gradient of 22 T/m for $I = 1000A$, with a corresponding peak coil field of the order of 1.3 T (that is only slightly higher than the magnetic field of $22 \times 0.05 = 1.1$ T reached at the magnet inner radius of 5 cm).

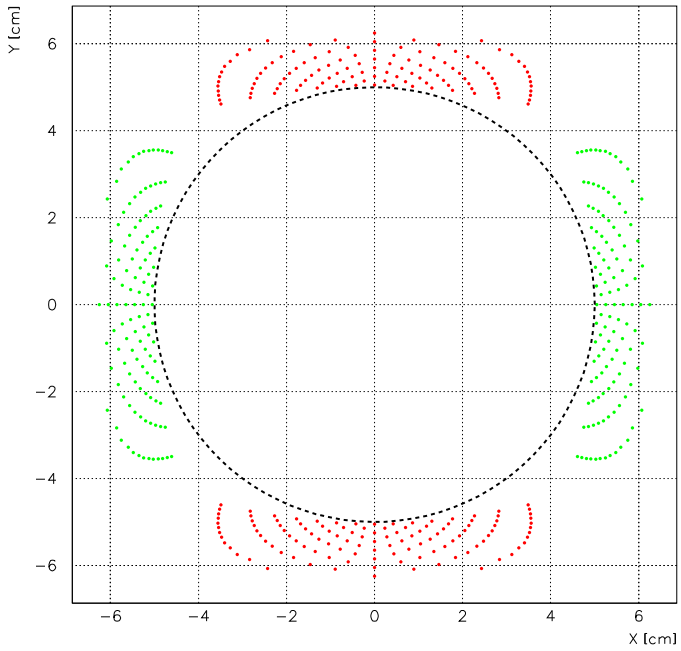

Figure 7: Bipolar-current quadrupole magnet made of 13 layers of 60, 56, ... and 12 wires, respectively. The green wires are of positive current while the current is negative in the red wires. The inner aperture of the magnet and the minimum inter-layer distance have been adjusted to 5 cm and 1 mm, respectively. This magnet produces a pure quadrupole field with C_{14} the first non-zero harmonics after C_2. Its transfer function is about 22 T/m/kA with a peak coil field of 1.3 T assuming a current of $I = 1000$ A.

4 Single aperture magnets generating a more exotic magnetic field with specified multipole expansions at more than one location of the transverse plane

In this last section, a few examples will illustrate the more delicate case of a magnetic field for which the multipole expansion is prescribed at several locations of the transverse plane. We will start with the so-called "sextupole-like quadrupole" mentioned in the introduction of this paper. Then in sub-sections 4.2, we will study the possibility of designing mass-less septa and two-jaw magnetic collimators, that is defining the layout of a single aperture magnet for which the multipole expansion of the field is vanishing up to an order M at a given point of the transverse aperture and can be approximated by a pure dipole field around one or two other locations.

4.1 The "sextupole-like quadrupole"

As already mentioned in the introduction, the overall study has been motivated by the design of a single aperture magnet able to produce a pure quadrupole field, say up to the order $M = 10$, which would change sign around two specified positions$\pm x_0$ of the transverse plane:

$$\begin{cases} \mathbf{B}(x_0 + z) &= B_2\, z + \mathbf{O}(z^M) \\ \mathbf{B}(-x_0 + z) &= -B_2\, z + \mathbf{O}(z^M)\,. \end{cases} \tag{61}$$

As discussed in section 2.3.2 (paragraph "$P = 2$"), the minimum number of wires needed is equal to $2M$ for bipolar systems, that is 20 wires in our specific case. The transverse positions

of these wires are then given by the $2 \times M$ complex roots of two polynomials $Q_\pm$, each of degree M and fulfilling the following conditions (see Eq. (26)):

$$\left\{ \begin{array}{rcl} Q_+(z+a) & \propto & Q_-(z+a) \times \exp(B_2\, z^2/2) + \mathbf{O}(z^{M+1}) \\ Q_+(z-a) & \propto & Q_-(z-a) \times \exp(-B_2\, z^2/2) + \mathbf{O}(z^{M+1}) \end{array} \right. \tag{62}$$
$$\text{with } \deg(Q_\pm) = M \text{ and } Q_\pm(0) = 1\,.$$

As shown in section 2.3.2, the determination of these two polynomials is equivalent to an eigenvalue problem. More precisely, using vector notations (see Eq. (33)), the polynomial Q_+ normalised to $Q_+(0) = 1$ is an eigen-vector of the $(M+1)\times(M+1)$ square matrix defined by

$$A \overset{\text{Eq.(35)}}{=} T_{-x_0}\, A_1\, T_{x_0}^2\, A_2^{-1}\, T_{-x_0}\,, \tag{63}$$

while the polynomial Q_- is obtained by the following relation

$$Q_- \overset{\text{Eq.(34)}}{=} \mathbf{cst} \times \left[T_{x_0}\, A_2^{-1}\, T_{-x0}\right]\, Q_+\,, \tag{64}$$

where the multiplicative constant on the right-hand side is fixed by the condition $Q_-(0) = 1$. In the above two equations, $T_{\pm x_0}$ denote the matrices associated to the linear operators of translation $\mathcal{T}_{\pm x_0}$ acting on the ring $\mathsf{C}_M[z]$ of the polynomials of degree equal or lower than M (see the definition (30) and Eq. (31)). Then, the matrices $A_{1,2}$ describe the operators of multiplication $\mathcal{A}_{R_1,R_2}$, up to the order M, by the functions $R_{1,2} \overset{\text{def}}{=} \exp(\pm B_2\, z^2/2)$ (see Eq.'s (28) and (29)). Using the symmetries which are intrinsic to this particular case, the problem can be somehow simplified by remarking that

$$R_1(z) \times R_2(z) \equiv 1 \Rightarrow A_2^{-1} = A_1\,, \tag{65}$$

and by introducing the symmetry operator $\mathcal{V}$ defined by

$$\begin{array}{rccc} \mathcal{V}: & \mathsf{C}_M[z] & \longrightarrow & \mathsf{C}_M[z] \\ & Q(z) & \mapsto & Q(-z)\,. \end{array} \tag{66}$$

Indeed, in the usual basis $(1, z, \ldots, z^M)$, the matrix V associated to the operator $\mathcal{V}$ is diagonal and given by

$$V = \mathbf{Diag}(1,\, -1,\, \ldots,\, 1,\, -1) \text{ (assuming } M \text{ is an even number for the sake of simplicity).} \tag{67}$$

Furthermore, the matrix V possesses the following properties:

$$\left\{ \begin{array}{rcl} V^2 & = & \mathbf{1} \\ V\, T_{\pm x_0}\, V & = & T_{\mp x_0} \\ V\, A_{1,2}\, V & = & A_{1,2}\,, \end{array} \right. \tag{68}$$

where the first two properties are obvious, for instance by coming back to the basic definition of the operators $\mathcal{V}$ and $\mathcal{T}_{\pm x_0}$, and where the last property comes from the parity of the functions $R_{1,2} \overset{\text{def}}{=} \exp(\pm B_2\, z^2/2)$ with respect to the z-variable. Using these properties, the matrix A to be diagonalized can then be re-expressed as follows:

$$\begin{array}{c} A \overset{\text{Eq.(63)}}{=} T_{-x_0}\, A_1\, T_{x_0}^2\, A_2^{-1}\, T_{-x_0} \overset{\text{Eq.(65)}}{=} T_{-x_0}\, A_1\, T_{x_0}^2\, A_1\, T_{-x_0} \equiv B^2 \\ \text{with } B \overset{\text{def}}{=} T_{-x_0}\, A_1\, T_{x_0}\, V \overset{\text{Eq.(68)}}{=} V\, T_{x_0}\, A_1\, T_{-x_0}\,. \end{array} \tag{69}$$

Any eigenvector of the matrix B is then an eigenvector for the matrix A and conversely if the B matrix has $M+1$ distinct eigenvalues, that is in particular $M+1$ linearly independent eigenvectors, which is generally the case in practice. The polynomials Q_+ can therefore be searched as an eigen vector of the matrix B:

$$[T_{-x_0}\, A_1\, T_{x_0}\, V]\, Q_+ \equiv \lambda Q_+ \text{ with } Q_+(0)\text{=1 for the normalization,} \tag{70}$$

which in principle possesses $M+1$ distinct solutions. Then, the relation (64) can be used to determine the polynomial Q_-:

$$\begin{array}{cccc} Q_- & \overset{\text{Eq.(64)}}{=} & \mathbf{cst} \times \left[T_{x_0}\, A_2^{-1}\, T_{-x0}\right]\, Q_+\,, & \overset{\text{Eq.(65)}}{=} \quad \mathbf{cst} \times [T_{x_0}\, A_1\, T_{-x0}]\, Q_+ \\ & \overset{\text{Eq.(68)}}{=} & \mathbf{cst} \times [V\, T_{-x_0}\, A_1\, T_{x0}\, V]\, Q_+ & \overset{\text{Eq.(70)}}{=} \quad \lambda \times \mathbf{cst} \times V\, Q_+\,. \end{array} \tag{71}$$

Finally, using the normalization condition $Q_\pm(0) = 1$, we get $\lambda \times \mathbf{cst} \equiv 1$, which simply means that in the bipolar-current configuration the so-called "sextupole-like quadrupole" shall exhibits a dipolar symmetry:

$$Q_-(z) = Q_+(-z)\,. \tag{72}$$

All this being said, we then expect $M+1$ different possible wire configurations to achieve a prescribed sextupole-like quadrupole field up to the order M. These configurations are shown in Fig. 8 in the case $M = 10$, $x_0 = 1$ cm and $B2 = 50'000$ corresponding to a magnet transfer function of 10 T/m/kA. Only one of these 11 possible solutions does not exhibit any wire in the magnet mid-plane. This solution is illustrated in more detail in Fig. 9, in particular in terms of field lines and 2D-mappings of the vertical and horizontal field as a function of x and y. The region of good field quality does not extend beyond a radius of about $x_0/2$ around the two transverse positions $\pm x_0$ where the produced magnetic field has been specified to be purely quadrupolar up to the order $M = 10$. This feature might be non-limiting to cope with two circulating round beam, say collimated at 3σ and separated by $2\,x_0 \sim 10\sigma$. This represents however a first severe bottleneck for our present purpose where the initial goal was to produce flat beams at the interaction point and to separate them in the plane of smallest $\beta_{\max}$ (see Section 1). The second limitation occurs when trying to push the magnet transfer function applying for instance the radial stacking strategy described in sub-section 3.5.1. More precisely, Fig. 10 shows a multi-layers sextupole-like quadrupole magnet obtained by keeping $x_0 = 1$ cm and M=10, but solving our problem for several successive values for B_2 decreasing from $B_2^{(\max)} = 50'000$ to $B_2^{(\min)} = 500$. While some wires tends to moves away from the origin (the 2+2 wires on the left/right side of each pictures), the mid-plane of the magnet exhibits 4 and then 8 accumulation points where the other wires tends to concentrate.
To summarise, we conclude that sextupole-like quadrupole magnets can certainly be achieved but exhibit specific features and/or serious limitations in terms of geometry and/or maximum possible gradient to be of any interest for the upgrade of the LHC experimental insertions.

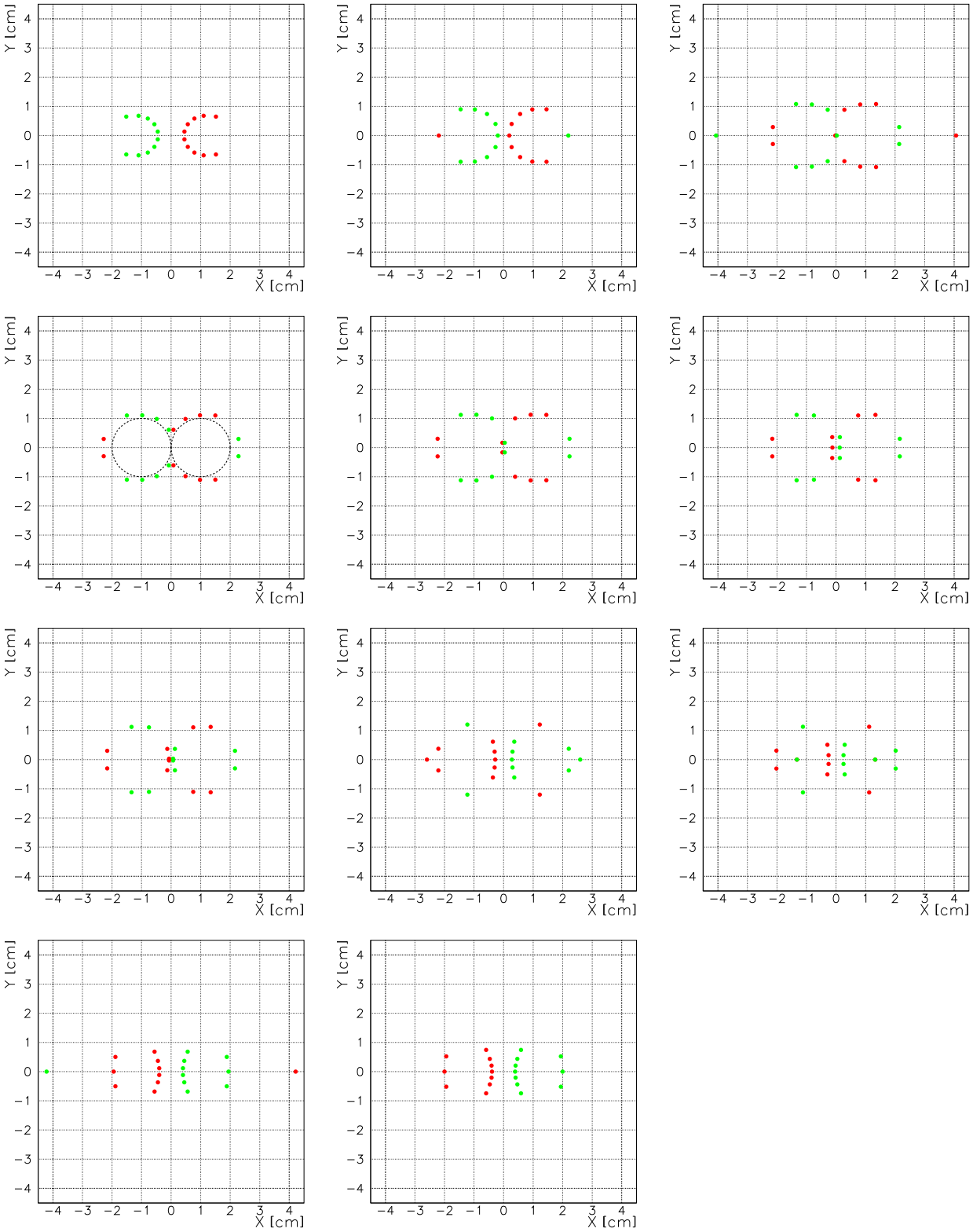

Figure 8: Eleven possible wire configurations generating the sextupole-like quadrupole field described by Eq. (61) with $M = 10$, $x_0 = 1$ cm and $B_2 = 50'000$ (green and red wires are of positive and negative current, respectively). Starting from the top, the fourth configuration offers the widest aperture (no wire in the vicinity of the magnet center).

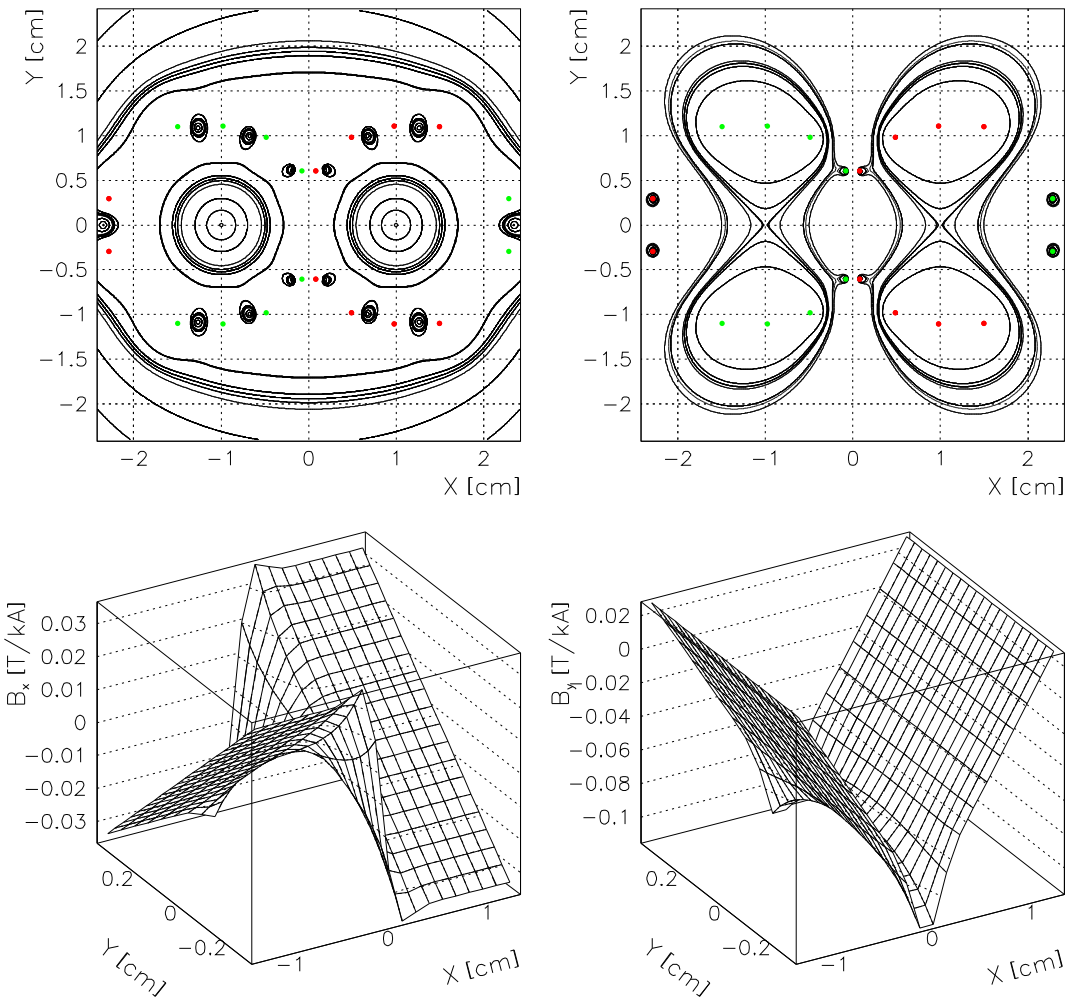

Figure 9: "Sextupole-like quadrupole" magnet obtained for $M = 10$, $x_0 = 1$ cm and $B_2 = 50'000$ corresponding to a transfer function of 10 T/m/kA: contours of constant magnitude of $\mathbf{B}$ (top-left), line of $\mathbf{B}$ (top-right) and $B_{x,y}$ field maps (bottom-left and bottom-right pictures respectively).

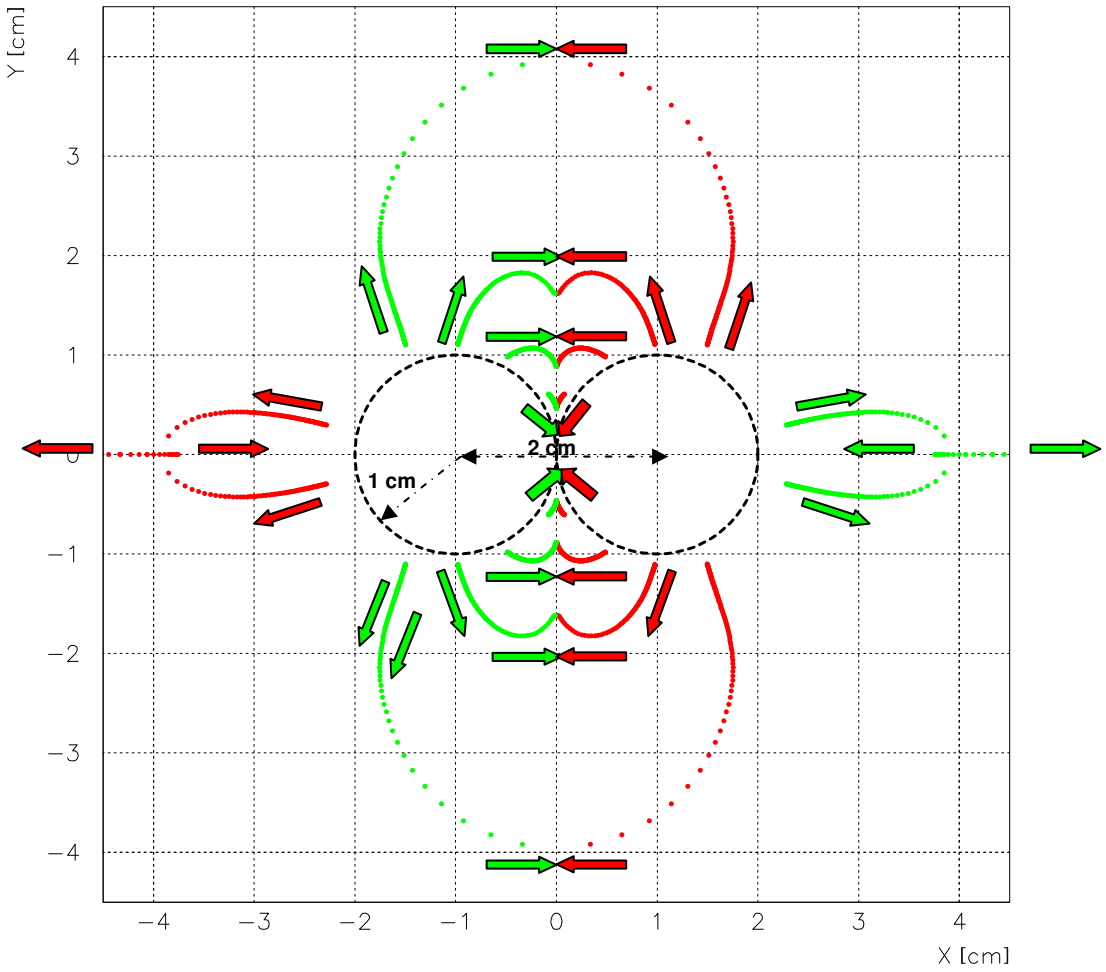

Figure 10: Multi-layer "sextupole-like quadrupole" obtained for $M = 10$, $x_0 = 1$ cm and several values of B_2 decreasing from 50'000 to 500. As usual, the wires of positive current are indicated in green and those of negative current in red. The green and red arrows illustrates the change of position of the corresponding wires when B_2 is reduced.

4.2 The mass-less septum and the two-jaw magnetic collimator

As final examples, we will investigate the case of a mass-less septum and of a two-jaw magnetic collimator, that is a magnetic field specified at two or three locations of the transverse plane, $Z_{1,2} = (0,\, x_0)$ or $Z_{1,2,3} = (0,\, x_0,\, -x_0)$, and possessing the following characteristics:

$$\begin{array}{lll} \text{Case 1:} & \mathbf{B}(x_0 + z) = B_1 + \mathrm{O}(z^{M+1}) & \text{and} \quad \mathbf{B}(-x_0 + z) = \mathrm{O}(z^{M+1}) \\ \text{Case 2:} & \mathbf{B}(\pm x_0 + z) = \pm B_1 + \mathrm{O}(z^{M+1}) & \text{and} \quad \mathbf{B}(z) = \mathrm{O}(z^{M+1})\,, \end{array} \tag{73}$$

with B_1 defining the magnitude of the vertical dipole field in the region(s) which is (are) adjacent to the zero-field region.

Contrary to the "sextupole-like quadrupole magnet", the problem will be solved assuming the current I to be positive for all the wires (unipolar system). According to section 2.3.1, the minimum number of wires needed is equal to $2 \times M$ and $3 \times M$ in these two respective cases. Their transverse positions is then given by the complex roots of the polynomial Q_+ which is

univocally determined by the following condition (see Eq. (13)):

$$\text{Case 1:} \quad \frac{Q_+(x_0+z)}{Q_+(x_0)} = \sum_{k=0}^{M} \frac{B_1^k z^k}{k!} + \mathrm{O}(z^{M+1}) \qquad \text{and} \quad \frac{Q_+(-x_0+z)}{Q_+(-x_0)} = 1 + \mathrm{O}(z^{M+1})$$

$$\text{Case 2:} \quad \frac{Q_+(\pm x_0+z)}{Q_+(\pm x_0)} = \sum_{k=0}^{M} (\pm)^k \frac{B_1^k z^k}{k!} + \mathrm{O}(z^{M+1}) \quad \text{and} \quad \frac{Q_+(z)}{Q_+(0)} = 1 + \mathrm{O}(z^{M+1})\,, \tag{74}$$

with $Q_+(0) = 1$ and $\deg(Q_+) = 2\,M\,/\,3\,M$ for case 1 and 2, respectively.
Taking in both cases $x_0 = 5$ cm and $B_1 = 50$, that is a transfer function of 100 G/kA, the corresponding unipolar-current magnets are shown in Fig.'s 11 and 12 for the 40-wires mass-less septum ($M = 20$) and the 56-wires magnetic collimator ($M = 18$), respectively.
Qualitatively speaking, the horizontal width of the transition region is about 2 cm in both cases, that is about 20% of the distance $2x_0$ separating the two extreme locations where the multipole expansion of the field has been specified. In the vertical direction, the region of good field quality extend up to $y = \pm 1 \rightarrow \pm 1.5$ cm in the case of the mass-less septum due to the presence of wires located at $(x,\, y) \sim (0,\, \pm 2\,\mathrm{cm})$. On the other hand, for the two-jaw collimator, this area does not extend beyond $y = \pm 0.5 \rightarrow \pm 0.7$ cm, leaving nevertheless three regions of extremely good field quality: the field free region containing the rectangular area defined by $\{|x| \leq 1.5$ cm, $|y| \leq 0.5$ cm$\}$ and the two dipole field regions defined by $\{-5.5$ cm$\leq x \leq -4$ cm, $|y| \leq 0.5$ cm$\}$ and $\{4$ cm$\leq x \leq 5.5$ cm, $|y| \leq 0.5$ cm$\}$ (see Fig. 13 for more details).
Without going into the details, it is worth mentioning that as for the "sextupole-like quadrupole magnet", any attempt to increase the transfer function of these magnets (e.g. via the radial stacking strategy described in section 3.5.1) tends to generate wire accumulation points close to the magnet mid-plane. In other words, such magnets do not appear very attractive in terms of maximum achievable transfer function, which may limit their potential use in high-energy beam extraction lines. On the other hand, the latter remain rather interesting objects to be used as primary collimators in high-energy ring, e.g. by injecting in the wires an AC-current tuned to the betatron frequency. Indeed, in a multi-turn process, this will tend to clean the transverse tails of the beam while minimizing the diffusion effects generated in its core. This proposal will form the subject of a future study.

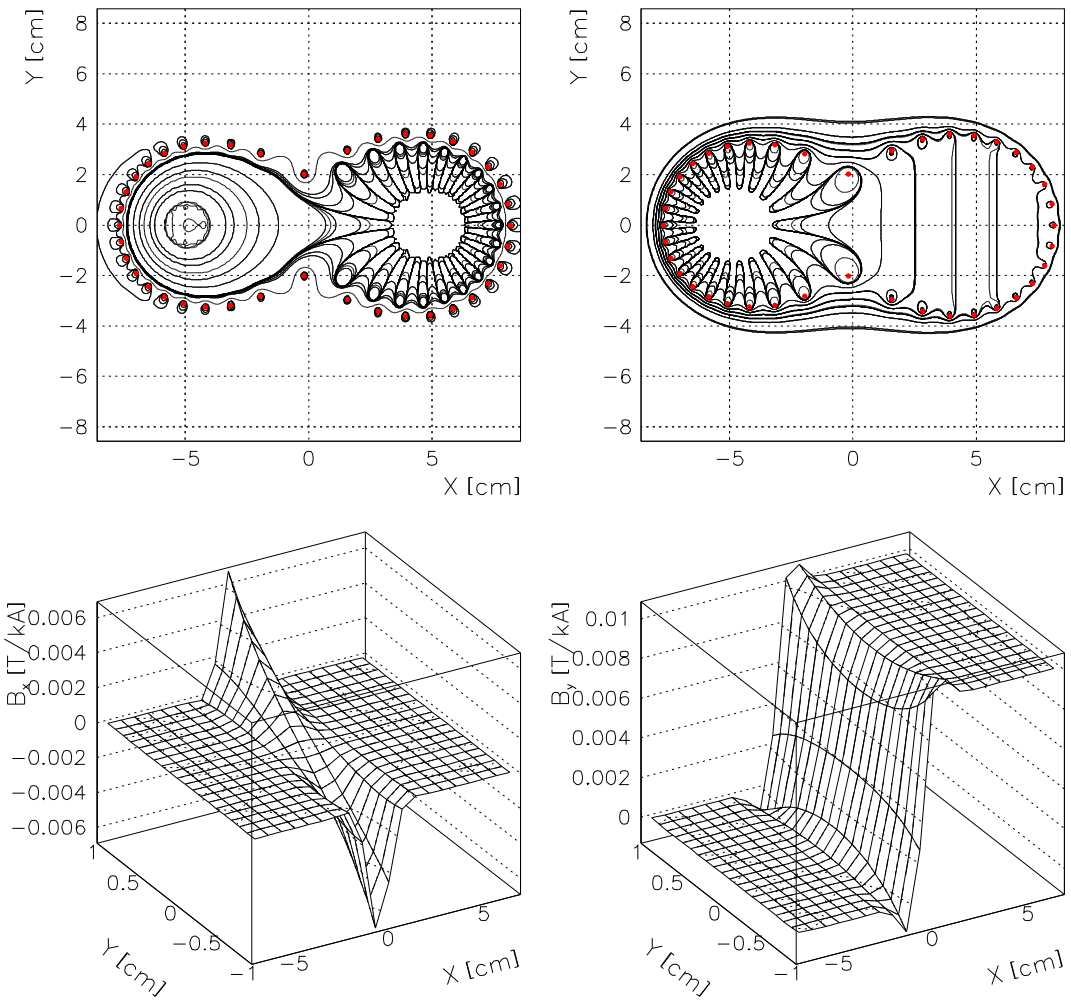

Figure 11: Unipolar-current mass-less septum made of $2 \times M = 40$ wires and corresponding to $B_1 = 50$ (i.e. transfer function of 100G/kA) and $x_0 = 5$ cm in Eq. (73) (case 1): contours of constant magnitude of $\mathbf{B}$ (top-left), lines of $\mathbf{B}$ (top-right) and $B_{x,y}$ field maps (bottom-left and bottom-right pictures respectively).

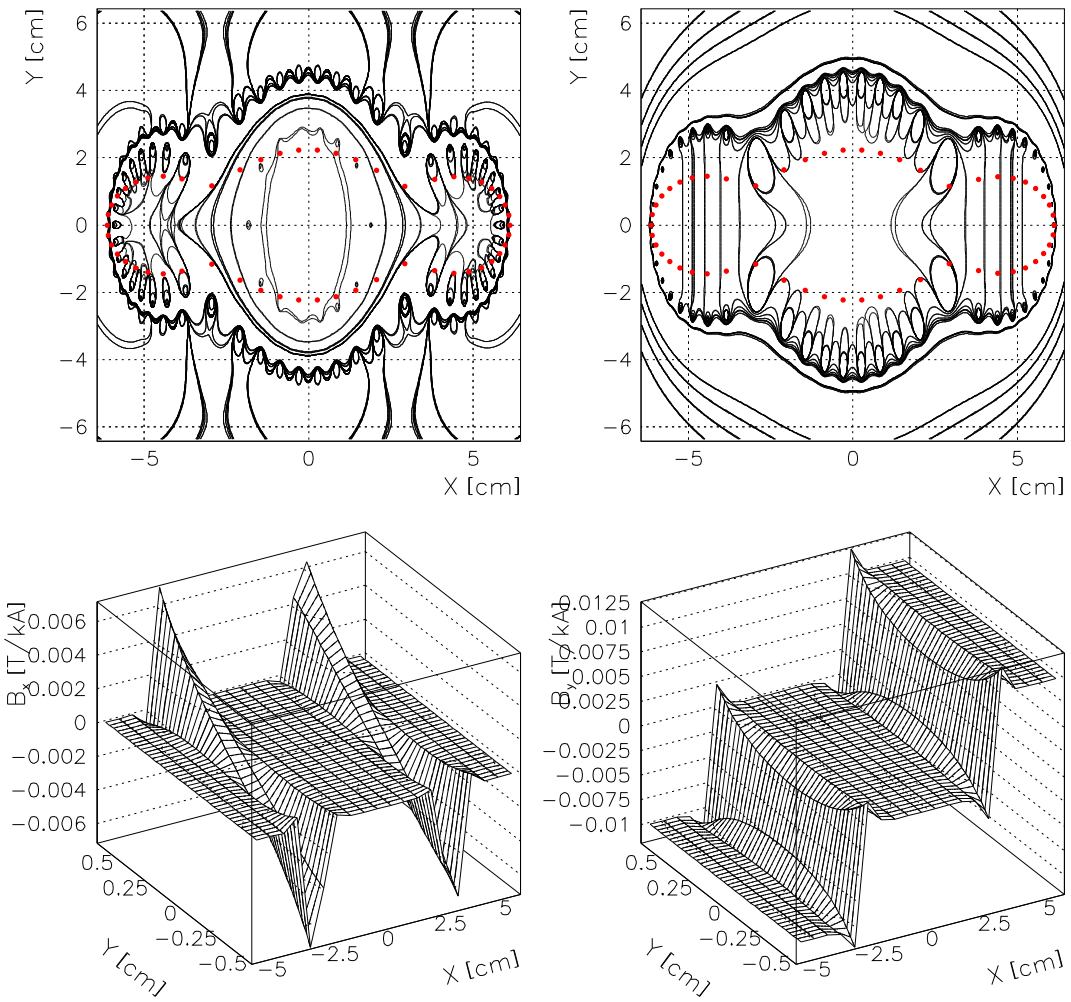

Figure 12: Unipolar-current two-jaw magnetic collimator made of $3 \times M = 54$ wires and corresponding to $B_1 = 50$ (i.e. transfer function of 100G/kA) and $x_0 = 5$ cm in Eq. (73) (case 2): contours of constant magnitude of $\mathbf{B}$ (top-left), lines of $\mathbf{B}$ (top-right) and $B_{x,y}$ field maps (bottom-left and bottom-right pictures respectively).

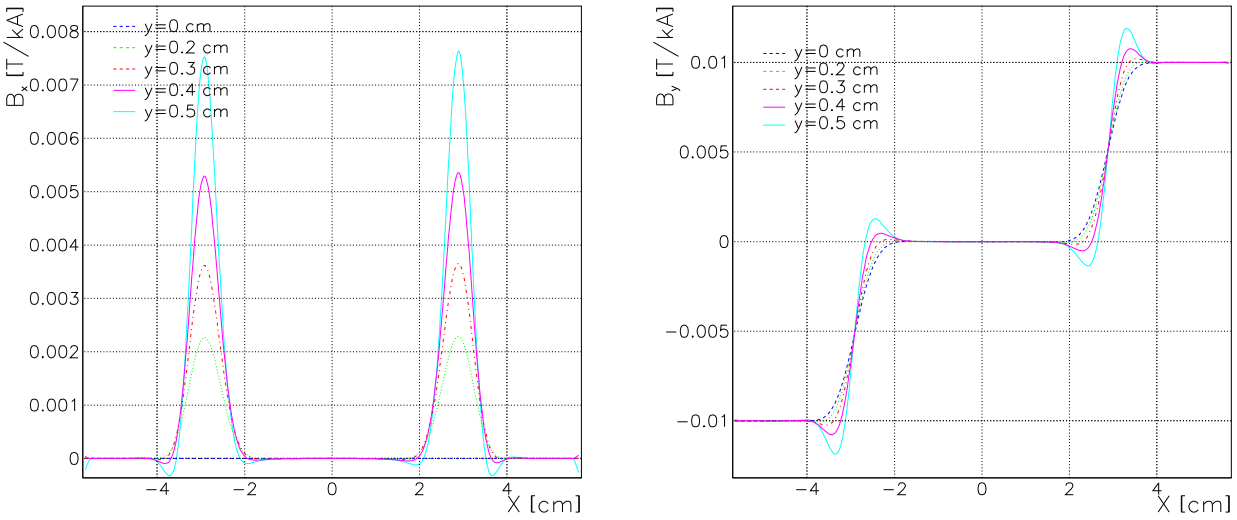

Figure 13: Horizontal (left picture) and vertical (right picture) magnetic field [T/kA] produced by the two-jaw magnetic collimator described in Fig. 12.

5 Summary and Conclusions

The first motivation of this paper has been the feasibility study of a mass-less focusing-defocusing quadrupole magnet, or "sextupole-like quadrupole magnet", in order to enhance the LHC luminosity while sticking to the so-called "quadrupole-first scenario" (see section 1 for more details). While principle designs of such a magnet can be obtained, the initial goal has not been reached in terms of maximum achievable gradient which would be useful for the LHC insertions (see section 4.1 for more details). On the other hand, this study allowed to set up a new algorithmic method able to generate in a deterministic way the distribution of N current wires which is associated to a given 2D-magnetic field (see section 2 for a detailed description). More precisely, as shown by the various examples and discussions presented in sections 3 and 4, it is clear that the method developed allows to design and study rapidly a given magnet which has been specified in terms of mechanical acceptance, field quality and characteristics of its main field at one or a several locations of its inner aperture. In particular, it allows to exclude or motivate quickly the detailed study of very exotic magnets, like the high-gradient sextupole-like quadrupole mentioned above or the single or two-jaw collimator described in section 4.2.
Furthermore, even if the solutions given are expressed in terms of filamentary current distributions, which is not practical for designing realistic high-field magnets, the potential of the method lies also in its possible connection to more standard magnet design programs. Indeed, working with conductor blocks and generally using algorithms of iterative type, these programs have generally no specific guaranties of convergence if, at the first iteration, the centroids of the coil-blocks is badly positioned. The method developed offers then this first iteration.
Finally, the connection with 2D-electrostatic field is straightforward, which gives another potential application of the method in the field of electrostatic magnets or wire chambers for particle detection.

Acknowledgments

I would like to warmly thank M. Giovannozzi for carefully reading this manuscript as well as my group leader for motivating me to pursue this study up to its term, in particular to

document the method, while the goal initially pursued was rapidly demonstrated to be unreachable.

References

[1] T. Sen et al., "US-LARP progress on LHC IR upgrade", LHC Lumi05 workshop, Sept. 2005, Archidosso, Italy.

[2] O. Brüning, R. De Maria and R. Ostojic, "Low gradient, large aperture IR upgrade options for the LHC compatible with Nb-Ti magnet technology", LHC-Project Report 1008, CERN, Geneva, Switzerland, July 2007.

[3] James T. Crow, "Unipolar-current dipoles and other optimum reduced-symmetry multipoles", J. Appl. Phys. **82**, pp. 1511-1517, Aug. 1997.

[4] T. Obana et al., "Prototype superconducting magnet for the FFAG accelerator", Fusion Engineering and Design 81 (2006), pp. 2541-2547.